EUROPEAN CENTRAL BANK
EUROSYSTEM

Working Paper Series

Claus Brand, Gavin Goy, Wolfgang Lemke

Estimating the natural rate of interest in a macro-finance yield curve model

No 3160

Abstract

Using a novel macro-finance model we infer jointly the equilibrium real interest rate r_t^*, trend inflation, interest rate expectations, and bond risk premia for the United States. In the model r_t^* plays a dual macro-finance role: as the benchmark real interest rate that closes the output gap and as the time-varying long-run real interest rate that determines the level of the yield curve. Our estimated r_t^* declines over the last decade, with estimation uncertainty being relatively contained. We show that both macro and financial information is important to infer r_t^*. Accounting for the secular decline in interest rates renders term premia more stable than those based on stationary yield curve models.

A previous version of this paper by the same authors entitled "Natural rate chimera and bond pricing reality" has been published as ECB Working Paper No 2612.

Keywords: Equilibrium real rate, natural interest rate, arbitrage-free Nelson-Siegel term structure model, term premia, Bayesian estimation.

JEL Classification: E43, C32, E52, C11, G12.

Non-technical summary

We introduce a novel macro-finance model that addresses the "natural rate puzzle", a disconnect in the literature whereby macroeconomic and finance perspectives yield inconsistent estimates of the natural real rate of interest. From a macroeconomic standpoint, the natural rate of interest r_t^* is the real interest rate consistent with the economy operating at its potential and thereby constitutes an indicator for monetary policy, while in asset pricing, r_t^* serves as an anchor for interest rate expectations in the long run. We propose an integrated approach where r_t^* fulfills both roles simultaneously.

To integrate the macroeconomic and the financial perspective, our model features two key components: (1) a "macro module" that links r_t^* to output growth trends and a non-growth component, while modeling inflation expectations and the output gap dynamics through the IS curve and Phillips curve; and (2) an arbitrage-free affine Nelson-Siegel (AFNS) term structure model, where the equilibrium nominal short-term rate $i_t^* = r_t^* + \pi_t^*$ anchors the yield curve. The model is estimated using U.S. data (1961–2019) using Bayesian methods.

Our findings can be summarized as follows:

We identify a trend in r_t^* that is distinct from established approaches that suggests a steady decline. The model identifies a rise and fall in r_t^* over six decades, with lower levels in the 1960s, 1970s, and post-Global Financial Crisis. This behavior arises because the model endogenizes the real rate, making the real rate gap stationary, in contrast to models treating the real rate as exogenous.

Investing whether the interest rate gaps measured in terms of shorter or longer maturities matter for macroeconomic fluctuations, we find that longer-maturity (e.g., 10-year) real rate gaps explain output gaps better than traditional short-term measures, highlighting the relevance of the yield curve in macroeconomic dynamics.

Our r_t^* estimates are comparatively precise. The model provides more precise estimates of r_t^*, with narrower uncertainty bands (90% uncertainty bands are smaller than 3 percentage points) compared to the established semi-structural approach (8 percentage points).

Accounting for the stochastic trend in interest rates affects the estimated behavior of term premia. We find term premia exhibit more cyclical behavior rather than the persistent decline implied by stationary term structure models.

We demonstrate robustness of these results to model specification changes. For instance,

an alternative model specification featuring a shadow-rate adjustment for the zero-lower-bound period gives rise to the same r^* estimates as the baseline model. Pseudo real-time estimation of r^* reveals robustness of estimates over time, with limited variation in the posterior median point estimate of r^* for shorter samples.

By integrating macroeconomic and financial perspectives, the paper resolves the inconsistencies highlighted in prior studies and provides a unified framework for estimating r_t^*. The findings suggest that r_t^* serves as a critical anchor for both yield curve dynamics and macroeconomic stabilization. Future extensions of this research could include inflation-linked bonds or the impact from central bank asset purchase programs.

1 Introduction

The natural real rate of interest, r_t^* , plays a prominent role in macroeconomics and finance: from a macro perspective, it is the real interest rate consistent with the economy operating at its potential level; from a finance perspective, it is the expected short-term real rate in the far future and thus, together with long-term inflation expectations, an anchor for the expectation of nominal short-term rates (i_t^*) and the entire yield curve. The natural rate is, however, unobserved and needs to be inferred from a model. The literature has typically addressed these roles separately and the two approaches "can lead to very different estimates of the natural rates and risk premia and the associated historical interpretations and narratives" as stressed recently by Davis et al. (2024); a finding that they coin the "the natural rate puzzle".

We address this puzzle in a macro-finance model where the natural real rate of interest fulfills its dual role. The first component, the "macro module", defines r_t^* as the real rate of interest that closes the output gap asymptotically. The natural rate is linked to the trend in output growth and a non-growth component, similar as in Laubach and Williams (2003, hereafter LW). However, unlike their paper, we explicitly model and estimate trend inflation as well as model-consistent inflation expectations. The gap between the *ex-ante* real rate of interest and the natural real rate drives the output gap in the IS equation and, thereby, inflation through the Phillips-curve. The second component of our model is an arbitrage-free affine Nelson-Siegel (AFNS) term structure model with a level factor that incorporates a stochastic trend determined by the equilibrium nominal short-term rate i_t^* (r_t^* plus trend inflation, π_t^*). The slope and curvature factors, by contrast, are mean-reverting as suggested by statistical tests. The estimation of our integrated macro-finance model is based on quarterly data from 1961Q2 to 2019Q4 for the United States, using a Bayesian approach.

We report the following main results. First, our r_t^* estimates exhibit a distinct rise and fall over the past six decades, with a particularly steep decline following the Global Financial Crisis, as opposed to the steady decline reported by Holston et al. (2017, hereafter HLW), and more in line with Del Negro et al. (2017).[1]

[1] The literature broadly agrees on a general downward trend in r_t^* and its fall to levels around zero in the wake of the financial crisis. The literature also explores underlying, fundamental drivers across a wide range of different modeling approaches. While empirical approaches can accommodate a broad range of factors, especially when exploiting cross-country heterogeneity in slow-moving drivers (as in Carvalho et al., 2025), they are not easily amenable to structural interpretation. Conversely, structural models can capture the structural propagation of specific drivers, like aging or inequality, but cannot cover factors in a more encompassing manner. The drivers underlying r_t^* explored in the literature include lower productivity and potential output growth, a rise in risk

In particular, we estimate r_t^* to have been lower in the 1960s and 1970s and after the Global Financial Crisis than LW and HLW report. The associated real-rate gap exhibits more cyclical behavior, as the inclusion of an interest rate equation renders the difference between the ex ante real rate and the natural real rate stationary. In contrast, treating real interest rates as exogenous allows for large and persistent real rate and output gaps.

Second, our macro-finance yield curve model is a natural laboratory to explore whether longer-maturity real rate gaps in the IS curve would be statistically preferred over the one-period real rate gap in our baseline specification. Comparing the marginal likelihood of models with different maturities of that gap suggests that a long-term (around ten years) real rate gap is preferred over the standard short-term measure.

Third, in addition to a new time series of point estimates, we obtain several insights on inference about r_t^*. Regarding the information content of yields, macroeconomic and survey data for estimating r_t^*, historical data decompositions suggest that all are relevant. As regards estimation uncertainty, our natural rate path is surrounded by measurably narrower uncertainty than usually implied by the semi-structural approach originating from LW. In that original approach, filtering uncertainty for r_t^* estimates using US data can be as large as eight percentage points (Fiorentini et al., 2018), while we find less than three percentage points for the width of the 90% range of the posterior distributions. We also checked the robustness of our r_t^* estimates regarding the zero-lower-bound period: when switching to a "shadow-rate" specification of our model, the resulting natural rate series is more volatile but shows the same low-frequency variation as in our baseline model.

Fourth, similar to Bauer and Rudebusch (2020), we find that by accounting for trends in equilibrium rates, term premia exhibit more cyclical behavior, rather than a distinct trend decline as implied by stationary term structure models.

Finally, our main results are robust against a host of modifications such as pseudo real-time estimation, generalizations of the yield curve model or allowing for stochastic volatility.

aversion, declining growth rates in the working-age population, rising savings in anticipation of longer retirement periods (at global level), safe-asset scarcity, and possibly increasing inequality and firm profits. See, e.g. Caballero et al. (2017); Gourinchas and Rey (2019); Papetti (2019); Rachel and Summers (2019); Mian et al. (2020) among a wide range of studies. As our model estimates determinants of r_t^* as latent factors, it allows only indirect and heuristic insights into the role of low-frequency drivers of r_t^*. The demographic transition, for example, would be captured through indirect effects on potential output growth through lower working-age population growth and non-growth factors, such as higher savings in anticipation of longer retirement periods.

Related literature

The papers most closely related to ours are Davis et al. (2024) and Feunou and Fontaine (2021). Both papers also present joint arbitrage-free macro-finance models, incorporating r_t^* and term premia by building on Cieslak and Povala (2015), where yields are driven by the trend real rate, trend inflation and a risk premium factor. In Davis et al. (2024), the macro side features r_t^* as the sum of trend growth and a non-growth component like in our case, building on LW. But, while they treat the latter as stationary, we consider it to contain a trend as in LW to capture persistent imbalances between savings and investment. More importantly, and in contrast to Davis et al. (2024), we incorporate explicitly the business-cycle stabilizing role of r_t^* (i.e. r_t^* represents the real rate that closes the output gap). Feunou and Fontaine (2021) do incorporate this feature (by imposing HLW-style IS curve restrictions on their VAR) but eschew an explicit link of r_t^* to potential growth and other factors. On the finance side, Davis et al. (2024) infer r_t^* from the whole yield curve with their central measurement equation linking the average – across maturities – nominal bond yield at time t to (observed) trend inflation and trend growth, as well as an (unobserved) headwind factor and a cyclical risk premium component. In contrast, the relevance of bond yield information for estimating r_t^* is less explicit in Feunou and Fontaine (2021).[2] Regarding the estimation approach more generally, Davis et al. (2024) also use Bayesian techniques, while Feunou and Fontaine (2021) deploy a multi-step frequentist approach.

Our paper also relates to the macro-finance literature that estimates the full natural yield curve yet emphasizing to a lesser extent the (implicit) estimate of the natural short-term rate. While Imakubo et al. (2018) and Dufrénot et al. (2022) focus on Japan, Kopp and Williams (2018) and Brzoza-Brzezina and Kotłowski (2014) use US data like our paper.[3] Only Kopp and Williams (2018) discusses term premium implications, but they do not impose the no-arbitrage constraint as in our paper.

Finally, our paper also contributes to a growing literature that extracts long-run trends in interest rates mainly from macroeconomic information *or* from the yield curve. Approaches that are mainly macro-based include Laubach and Williams (2016); Del Negro et al. (2017);

[2] From the description of the paper and its annex, it looks like i_t^* and π_t^* paths (which then add up to r_t^* via an identity) are mainly inferred from long-horizon survey information, and bond yield equation parameters are estimated subsequently.

[3] All four papers use a Nelson-Siegel set-up but differ from each other by the degree of time variation of the natural yield curve and by how real rates affect the output gap. Like in our paper, in Kopp and Williams (2018) only the level factor contains a stochastic trend, while the natural slope and curvature are constant. The other papers, instead, also allow for stochastic trends in factors other than the level factor.

Johannsen and Mertens (2021); Zaman (2024); González-Astudillo and Laforte (2025). Some of them include selected bond yields in their information set but without cross-maturity no-arbitrage restrictions. Approaches featuring the yield curve, building on the 'shifting-endpoint' paper by Kozicki and Tinsley (2001), include Dewachter et al. (2014); Cieslak and Povala (2015); Christensen and Rudebusch (2019); Ajevskis (2020); Bauer and Rudebusch (2020); Abbritti et al. (2023) and Christensen and Mouabbi (2024), but their models are largely silent regarding the macro relevance of their r_t^* measures.

The paper is organized as follows: Section 2 describes the model, Section 3 data and estimation. Section 4 presents the results. Section 5 and the Appendix discuss model extensions, derivations, robustness and additional results.

2 The Model

Our macro-finance model integrates the semi-structural macroeconomic approach of estimating r_t^* by LW into an affine term structure model in the spirit of Christensen et al. (2011). Time is discrete with one period corresponding to one quarter. We focus here on the key equations, leaving the presentation of the full state space model to the Appendix A.1.

2.1 A semi-structural macro model

The IS curve, following LW, links the output gap $\tilde{x}_t$, defined as $\tilde{x}_t = x_t - x_t^*$, with x_t and x_t^* denoting log actual and log potential output, respectively, to the real interest rate gap $\tilde{r}_t$,

$$\tilde{x}_t = a_1\tilde{x}_{t-1} + a_2\tilde{x}_{t-2} + a_3\big(\tilde{r}_{t-1} + \tilde{r}_{t-2}\big) + \varepsilon_t^{\tilde{x}}. \tag{1}$$

The real rate gap $\tilde{r}_t = r_t - r_t^*$ is the difference between the ex-ante short-term real rate, r_t, and its natural counterpart r_t^*. Potential output x_t^* evolves according to

$$x_t^* = x_{t-1}^* + g_{t-1} + \varepsilon_t^{x^*}, \tag{2}$$

where g_t is the expected quarterly growth rate of potential output and $\varepsilon_t^{x^*}$ captures the unexpected part of potential output. The real natural rate r_t^* is the sum of the annualized expected

growth rate of potential output and a "catch-all", non-growth component, z_t, i.e.

$$r_t^* = 4g_t + z_t. \tag{3}$$

The z_t component indirectly captures effects such as saving-investment imbalances arising from longer retirement periods, as well as an increased demand for safe assets, (Del Negro et al., 2017), or other financial frictions. Both g_t and z_t follow a random walk with variances σ_g^2 and σ_z^2, respectively.

While (3) explicitly links r_t^* to potential output growth and to non-growth factors, these are, in turn, unobservable, allowing only indirect inference about their role as drivers of r_t^*. Specifically, the non-growth factor z_t will help closing the gap between the low-frequency components in real interest rates and growth, and r_t^* will be strongly affected by cross-equation relationships, like its business-cycle stabilization properties in (J.34) and the term-structure equations presented in Section 2.2 below.

For measuring ex ante real rates, the observed nominal short-term interest rate needs to be deflated by a measure of expected inflation. LW proxy inflation expectations by forecasts from an AR(3), whereas HLW use a trailing four-quarter average of inflation to approximate inflation expectations. In contrast, we define the ex ante real rate in a model-consistent manner as $r_t = y_t(1) - E_t\pi_{t+1}$, where $y_t(1)$ denotes the nominal yield of a one-quarter zero coupon bond and $E_t\pi_{t+1}$ is the conditional expectation of the one-period ahead inflation based on model dynamics.[4]

Our second main equation, the Phillips curve, is given by

$$\tilde{\pi}_t = b_1\tilde{\pi}_{t-1} + b_2\tilde{x}_{t-1} + \varepsilon_t^{\pi}, \tag{4}$$

where $\tilde{\pi}_t = \pi_t - \pi_t^*$, represents the inflation gap, i.e. the difference of inflation π_t from its trend π_t^* (also a random walk with innovation variance $\sigma_{\pi^*}^2$).[5] As a result, the real rate gap $\tilde{r}_t$ affects the cyclical component of inflation through its impact on the output gap. This specification differs from LW and HLW who also impose a unit root on inflation but eschew an explicit expression for

[4] A comparison of our model-implied CPI inflation expectations with the core PCE inflation expectations of HLW in the Appendix A.3 shows large consistency between both measures although inflation expectations based on core inflation are more stable over the second half of the sample. This result rules out that large and persistent differences in r_t^* estimates come from different measures of inflation expectations.

[5] The assumption of a random walk for trend inflation is shared with, e.g., Cogley and Sargent (2005); Stock and Watson (2007); Aruoba and Schorfheide (2011); Del Negro et al. (2017) to name but a view.

its stochastic trend. Specifically, their Phillips curve is formulated for inflation in levels (rather than inflation gaps) and coefficients of lagged inflation terms are constrained to sum to unity.

Relative to a canonical New Keynesian model, our Phillips curve is purely backward-looking. Adding a forward-looking element would substantially increase the computational burden in combination with the various non-stationary variables and the term structure component and also constitute a fundamental change in slower-moving macroeconomic stabilization properties of the model.[6]

2.2 Yield curve dynamics

We close the model by specifying the dynamics of the nominal risk-free yield curve. At each point in time, the cross section of yields of all maturities is assumed to be explained by three factors ("level", L_t, "slope", S_t, and "curvature", C_t) with factor loadings across maturities following the functional form of Nelson and Siegel (1987):

$$y_t(\tau) = \mathcal{A}(\tau) + L_t + \theta_s(\tau)S_t + \theta_c(\tau)C_t, \tag{5}$$

where $y_t(\tau)$ denotes the τ-quarter nominal bond yield, and factor loadings are given by

$$\theta_s(\tau) = \frac{1-\exp(-\lambda\tau)}{\lambda\tau} \text{ and } \theta_c(\tau) = \frac{1-\exp(-\lambda\tau)}{\lambda\tau} - \exp(-\lambda\tau). \tag{6}$$

An increase in the level factor induces a parallel upward shift of the whole yield curve, an increase in the slope factor increases the short end by more than the long end (hence, strictly speaking, "negative slope factor"), and an increase in the curvature factor accentuates the curvature at short- to medium-term maturities. The parameter λ governs how strongly a change in the slope factor S_t affects the slope of the yield curve and at which maturity the curvature factor has its maximum impact on the yield curve. The intercept term $\mathcal{A}(\tau)$ does not appear in the original Nelson-Siegel specification but is added to rule out arbitrage as described by Christensen et al. (2011) and detailed further in Appendix B.

We treat the level factor as non-stationary, while imposing stationarity on the slope and curvature factors, as suggested by unit root tests (Appendix C).[7] We thus decompose the level

[6] See Brand et al. (2018) for a detailed discussion of how modeling assumptions affect the stabilization properties of r_t^*.

[7] Del Negro et al. (2017) and Bauer and Rudebusch (2020) assume that also the slope is non-stationary, thus rendering term premia non-stationary. From an econometric perspective, such an assumption may fit the data

factor L_t into

$$L_t = L_t^* + \tilde{L}_t \tag{7}$$

where L_t^* is a non-stationary trend such that $\lim_{h\to\infty} E_t L_{t+h} = L_t^*$ and $\tilde{L}_t$ is a zero-mean stationary (or "cyclical") component. Using (5), the one-quarter short-term interest rate, $i_t = y_t(1)$, is given by

$$i_t = \mathcal{A}(1) + L_t + \theta_s(1)S_t + \theta_c(1)C_t, \tag{8}$$

with the limit

$$\lim_{h\to\infty} E_t i_{t+h} \equiv i_t^* = \mathcal{A}(1) + L_t^* + \theta_s(1)\bar{S} + \theta_c(1)\bar{C}, \tag{9}$$

where $\bar{S}$ and $\bar{C}$ denote the constant long-run means of the stationary slope and curvature factor, respectively. In combination with Equation (9), the long-run Fisher equation $i_t^* = \pi_t^* + r_t^*$ pins down the trend component of the level factor as $L_t^* = \pi_t^* + r_t^* - \theta_s(1)\bar{S} - \theta_c(1)\bar{C} - \mathcal{A}(1)$. As L_t^* is a latent process and $\mathcal{A}(1)$ is a free parameter (see Appendix B), we set $\mathcal{A}(1) = -\theta_s(1)\bar{S} - \theta_c(1)\bar{C}$ so that the long-run level factor is equal to the nominal short-term natural rate[8]

$$L_t^* = i_t^* \equiv r_t^* + \pi_t^*. \tag{10}$$

For the stationary, zero-mean, component of the level factor we specify an AR(1) process

$$\tilde{L}_t = a_L \tilde{L}_{t-1} + \varepsilon_t^{\tilde{L}}, \tag{11}$$

with $|a_L| < 1$. Finally, slope S_t and curvature C_t are assumed to follow a bivariate, stationary VAR that also includes the inflation and output gap as potential drivers:

$$S_t = a_{10} + a_{11}S_{t-1} + a_{12}C_{t-1} + a_{13}\tilde{\pi}_{t-1} + a_{14}\tilde{x}_{t-1} + \varepsilon_t^S, \tag{12}$$

$$C_t = a_{20} + a_{21}S_{t-1} + a_{22}C_{t-1} + a_{23}\tilde{\pi}_{t-1} + a_{24}\tilde{x}_{t-1} + \varepsilon_t^C. \tag{13}$$

The inclusion of the gap measures highlights the cyclical nature of slope and curvature.[9] Alter-

equally well, and Bauer and Rudebusch (2020) assert that "...the estimated term premium with a shifting endpoint exhibits more pronounced cyclical variation, in line with the notion that risk premia are countercyclical [...]", underlining that the stationarity vs. non-stationarity of term premium and slope is probably a borderline case.

[8] Other choices, e.g. $\mathcal{A}(1) = 0$ would have induced a constant wedge between L_t^* and i_t^* but would not affect the model property that shifts in i_t^* translate one-for-one to shifts in the natural level L_t^*.

[9] Note that the assumption of yield curve factors following a first order VAR is standard in the literature, with

natively specifying a more general trivariate VAR for the stationary yield curve factors does not change the results.[10]

The resulting model implies a "natural yield curve" at each point in time, i.e., maturity-specific attractors for all yields. To see this, take the limit of Equation (5) to find

$$\lim_{h\to\infty} E_t y_{t+h}(\tau) \equiv y_t(\tau)^* = \mathcal{A}(\tau) + L_t^* + \theta_s(\tau)\bar{S} + \theta_c(\tau)\bar{C}, \qquad \forall \quad \tau \in \mathbb{N}^+. \tag{14}$$

The "natural slope" for any maturity τ, $y_t^*(\tau) - y_t^*(1) = \mathcal{A}(\tau) + \theta_s(\tau)\bar{S} + \theta_c(\tau)\bar{C}$, is time invariant, because the short-term natural real rate and trend inflation equally affect the short and long end of the natural yield curve. Hence, the *location* of the natural yield curve varies over time, while the long-run *shape* of the natural yield curve is time-invariant.

Although we cannot use the difference between the nominal natural and observed yield curves as a measure of the monetary policy stance *stricto sensu* (since this would require an estimate of the *real* natural yield curve[11]), extending the concept of the natural rate to the entire yield curve provides a useful benchmark for whether, at each point in time, the actual nominal natural yield curve is close to its estimated long-run level or whether one would expect adjustments towards it over time. Appendix G presents estimates of the natural yield curve at different points in time and their interpretation.

We compute the term premium of maturity τ, denoted $TP_t(\tau)$, as the difference between the model-implied τ-period bond yield, $\hat{y}_t(\tau)$ and its expectations component, i.e. the expected average of future short rates over the respective maturity:

$$TP_t(\tau) = \hat{y}_t(\tau) - \frac{1}{\tau}\sum_{h=0}^{\tau-1} E_t(i_{t+h}). \tag{15}$$

As the short rate is a function of yield curve factors (8), their dynamics pin down model-consistent expectations $E_t(i_{t+h})$ for all relevant horizons h. Forward term premia are computed

several papers adding unspanned macro factors to further inform the dynamics of yield curve factors. In contrast to Bauer and Rudebusch (2020), however, we do not allow the level factor (and thus i_t^*) to load on either slope or curvature, as this would render them non-stationary, contradicting the evidence presented in Section C of the Appendix.

[10] In this case, also the cyclical level factor is a function of lagged gap measures. Appendix J.5 shows that results are virtually unchanged but come at the cost of additional parameters.

[11] In Section 5.1 we show that it is intricate to compute model-consistent long-term real rates: first, computing the term structure of inflation expectations requires solving a fixed-point problem with some small modifications to the model; second, even when deflating nominal yields with thus-computed inflation expectations, the resulting real rates would still include inflation risk premia.

analogously.

Expectations $\sum_{h=0}^{\tau-1} E_t(i_{t+h})$ are linked to r_t^* and inflation expectations and thereby non-stationary. As both expected and observed yields embody the same trend i_t^*, their difference, the term premium, is stationary and converges to a constant mean. That is, the term structure of term premia has a time-invariant attractor $\lim_{h\to\infty} E_t\big[TP_{t+h}(\tau)\big] = TP^*(\tau)$.

2.3 Adding survey information

To help identify latent variables, we add survey information as observables.[12] Specifically, we include the Federal Reserve's series for perceived target inflation (PTR), as in e.g. Bauer and Rudebusch (2020), to measure expectations of average inflation over long horizons $E_t^s \pi_{t+\infty}$. We match it with trend inflation π_t^* plus a measurement error:

$$E_t^s \pi_{t+\infty} = \pi_t^* + u_t^{s,\pi}, \quad u_t^{s,\pi} \sim \mathcal{N}(0, \sigma_{s,\pi}^2). \tag{16}$$

To help measure near-term interest rate expectations, we also match Consensus survey expectations of short-term rates four quarters ahead, $E_t^s y_{t+4}(1)$, with the corresponding model-implied expectation plus a measurement error:

$$E_t^s y_{t+4}(1) = \mathcal{A}(1) + E_t L_{t+4} + \theta_S(1) E_t S_{t+4} + \theta_C(1) E_t C_{t+4} + u_t^{s,sr}, \quad u_t^{s,sr} \sim \mathcal{N}(0, \sigma_{s,sr}^2). \tag{17}$$

3 Methodology and Estimation

3.1 Data

The model is estimated over the sample period 1961Q2–2019Q4 using quarterly US data on log real GDP, year-on-year changes in the log consumer price index, nominal risk-free zero coupon yields for $K = 13$ maturities (1-4 quarters and 2-10 years), and surveys on inflation and interest rate expectations. Inflation (`CPIAUCSL`) and real GDP (`GDPC1`) data are both seasonally adjusted and taken from the FRED database of the Federal Reserve Bank of St. Louis. Nominal yields are end-of-quarter and based on the daily factors from Gürkaynak et al. (2007). The Federal Reserve's series for perceived target inflation (`PTR`), from the Federal Reserve's FRB/US

[12] The inclusion of survey data is common in both the literature that extracts low-frequency dynamics from macroeconomic time series (see, among others, Del Negro et al., 2015, 2017; Mertens, 2016; Mertens and Nason, 2020) and the literature on term structure modeling (see, e.g., Kim and Wright, 2005; Geiger and Schupp, 2018).

database, starts in 1968Q1. The Consensus Economics forecast of the 3-month T-Bill, 1-year ahead, starts in 1990Q1.

3.2 Methodology

As common in Bayesian estimation of unobserved components models, we use the Gibbs sampler and the Durbin and Koopman (2002) simulation smoother to jointly estimate potential output growth, output gap, trend inflation and real equilibrium interest rates. Our approach allows simultaneous estimation of all model parameters and latent states and eschews the multistep maximum likelihood approach adopted by HLW. The latter approach, drawing on the median unbiased estimation method proposed in Stock and Watson (1998), would be impractical for a model of this size.[13]

Specifically, the Gibbs sampler generates draws from the joint posterior distribution of states ξ_t, the DNS parameter λ and all other parameters θ, given the observables ζ, denoted $p(\xi, \theta, \lambda|\zeta)$. As the measurement equations depend on λ in a nonlinear fashion, we cannot sample from its distribution directly. Instead, we specify a random walk Metropolis Hastings step for λ to approximate its conditional posterior. The Markov Chain Monte Carlo (MCMC) algorithm is explained in detail in Appendix D.

Finally, including survey data creates missing observations in the measurement equation because the surveys start only later in the sample. We therefore adapt the Durbin and Koopman simulation smoother to allow for missing values.[14]

3.3 Priors and posterior estimates

We use conjugate priors for all model parameters and variances, i.e. prior distributions are either Normal-Inverse-Gamma or Normal-Inverse-Wishart. For the parameters of the IS and Phillips curve, we position the sensitivity to real rate gap (a_3) and output gap (b_2) farther away from zero but otherwise center our prior means (for a_1, a_2 and b_1) around the estimates from LW. The AR(1) coefficient of the cyclical level factor is centered around 0.5 with a standard deviation of 0.25. For slope and curvature, our prior assumes that both follow a persistent AR(1) process with intercept, whose coefficients are based on OLS regressions of factors extracted from

[13] Buncic (2024) has recently criticized the multistep estimation approach by HLW for inconsistently implementing the mean unbiased estimation procedure by Stock and Watson (1998) and thereby generating a spuriously strong downward trend in the non-growth component of r_t^*.

[14] See Durbin and Koopman (2012), pp. 110-112, for details.

a standard DNS model. This prior allows for some shrinkage of all parameters in the VAR other than the own lag towards zero. Yet with a variance of $\sqrt{0.5}$, it is very loose.

The priors for the variances of the random walks are largely flat with scale and shape parameters equal to 4 and 2, respectively, which corresponds to a mean disturbance variance of 0.66 and a standard deviation of 0.47. The only exception is the variance of shocks to expected potential output growth σ_g^2. In principle, our prior choice prevents "pile-up" (convergence of σ_z^2 to zero).[15] Specifically, we choose shape and scale parameters of the Inverse-Gamma distribution such that its mean equals 0.0015, implying a priori variance of the change in (quarterly) potential output growth over one century of 0.6%. This prior ensures a fairly smooth estimate of trend growth, but leaves our r_t^* estimates unaffected.[16] A less informative prior instead causes trend growth g_t to exhibit stronger – and arguably implausible – cyclical dynamics, rendering the resulting output gap less persistent.[17]

For the DNS parameter λ, we assume a Normal prior with mean 0.1821 (the calibrated value in Diebold and Li (2006) adjusted for quarterly data) and a standard deviation of 0.1. The scale parameter of the random walk Metropolis Hastings algorithm is set to ensure an acceptance ratio between 20-40%. The Inverse-Wishart prior for the measurement errors of yields is centered around 0.5 and uninformative. Finally, we set the scale and shape parameters of the Inverse-Gamma priors for the inflation and short-term rate surveys to have a mean disturbance variance of 0.66 and a standard deviation of 0.47.

Table 3.1 summarizes the priors and posterior of the main structural parameters. In general, posterior distributions as additionally illustrated in the Appendix E suggest that all parameters are well identified from the data. The table also compares our posterior to the published estimates by HLW where applicable. Despite differences in the two studies across several important dimensions – including Bayesian vs. multi-step maximum likelihood estimation, closing the model with nominal yield dynamics or not, the specification of inflation dynamics, using survey information or not – the parameter estimates are broadly similar. However, the posterior median estimates of the loading coefficient of the real rate gap, a_3, in the IS equation and of the slope of the Phillips curve, b_2, are -0.2 and 0.14, respectively, and thus higher than those

[15] See the discussion in Kim and Kim (2013) on ARMA specifications for GDP (in their case with the likelihood surface of the MA-coefficient piling up at one).

[16] Section 5.3 discusses the sensitivity of results to a less tight prior.

[17] Davis et al. (2024) also impose a restriction on the joint dynamics of g and z, postulating that r_t^* and g are cointegrated, and imposing constraints on the "residual" z component. The key difference to us is the choice of z as being stationary.

Table 3.1: Prior and posterior densities of parameter estimates

		Prior		Posterior				
Parameter	Distr.	Mean	SD	Mean	Median	5%	95%	HLW
a_1	$\mathcal{N}$	1.50	0.25	1.40	1.42	1.13	1.61	1.53
a_2	$\mathcal{N}$	-0.6	0.25	-0.65	-0.65	-0.87	-0.42	-0.59
a_3	$\mathcal{N}$	-0.2	0.05	-0.2	-0.2	-0.27	-0.14	-0.07
b_1	$\mathcal{N}$	0.65	0.2	0.62	0.63	0.38	0.81	0.67
b_2	$\mathcal{N}$	0.15	0.05	0.14	0.14	0.07	0.21	0.08
a_L	$\mathcal{N}$	0.5	0.25	0.51	0.51	0.21	0.83	
a_{10}		$\begin{pmatrix} -0.24 \\ 0.85 \\ 0 \\ 0 \\ 0 \\ -0.3 \\ 0 \\ 0.78 \\ 0 \\ 0 \end{pmatrix}$		-0.54	-0.54	-0.93	-0.22	
a_{11}				0.69	0.69	0.57	0.79	
a_{12}				0.13	0.13	0.07	0.19	
a_{13}				0.00	-0.01	-0.12	0.11	
a_{14}	$\mathcal{MVN}$		$\sqrt{0.5} \cdot \mathbf{I_{10}}$	0.15	0.15	0.07	0.25	
a_{20}				-0.12	-0.10	-0.65	0.37	
a_{21}				0.33	0.33	0.18	0.49	
a_{22}				0.62	0.62	0.53	0.71	
a_{23}				-0.04	-0.04	-0.19	0.13	
a_{24}				-0.13	-0.13	-0.28	0.00	
σ_{Lc}	$\Gamma^{-1}(4,2)$	0.66	0.47	0.74	0.68	0.43	1.25	
σ_S	$\mathcal{W}^{-1}(2, \mathbf{I_2})$	2	$\mathbf{I_2}$	1.11	1.09	0.94	1.36	
σ_C				1.76	1.76	1.61	1.93	
σ_{π^*}	$\Gamma^{-1}(4,2)$	0.66	0.47	0.20	0.20	0.18	0.22	
σ_{x^*}	$\Gamma^{-1}(4,2)$	0.66	0.47	0.54	0.54	0.45	0.64	0.57
σ_g	Γ^{-1}	0.0015	2×10^{-7}	0.04	0.04	0.03	0.05	0.03
σ_z	$\Gamma^{-1}(4,2)$	0.66	0.47	0.32	0.32	0.27	0.37	0.16
$\sigma_{\tilde{\pi}}$	$\Gamma^{-1}(4,2)$	0.66	0.47	0.78	0.71	0.45	1.36	0.79
$\sigma_{\tilde{x}}$	$\Gamma^{-1}(4,2)$	0.66	0.47	0.76	0.70	0.43	1.30	0.35
$\sigma_{y(2)}$				0.24	0.24	0.22	0.26	
$\sigma_{y(3)}$				0.11	0.11	0.10	0.13	
$\sigma_{y(4)}$				0.10	0.10	0.09	0.11	
$\sigma_{y(8)}$				0.09	0.09	0.09	0.11	
$\sigma_{y(12)}$				0.08	0.08	0.07	0.08	
$\sigma_{y(16)}$	$\mathcal{W}^{-1}(15, \mathbf{I_{12}})$	0.5	∞	0.08	0.08	0.07	0.09	
$\sigma_{y(20)}$				0.08	0.08	0.07	0.09	
$\sigma_{y(24)}$				0.08	0.08	0.07	0.08	
$\sigma_{y(28)}$				0.07	0.07	0.07	0.08	
$\sigma_{y(32)}$				0.07	0.07	0.07	0.08	
$\sigma_{y(36)}$				0.08	0.08	0.07	0.09	
$\sigma_{y(40)}$				0.09	0.09	0.08	0.10	
$\sigma_{s,\pi}$	$\Gamma^{-1}(4,2)$	0.66	0.47	0.15	0.15	0.13	0.16	
$\sigma_{s,y(4)}$	$\Gamma^{-1}(4,2)$	0.66	0.47	0.13	0.13	0.12	0.15	
λ	$\mathcal{N}$	0.18	0.1	0.17	0.17	0.16	0.18	

Note: The table shows prior and posterior moments of the structural model parameters. The third and fourth column report the prior mean and standard deviation, with the corresponding shape and scale parameters for either inverse gamma or inverse Wishart distributions being reported in the second column. HLW refers to the published estimates from HLW from the New York Fed.

reported in HLW. They are above 0.1 in absolute terms – the critical threshold beneath which filtering uncertainty rises dramatically, as reported in Fiorentini et al. (2018).

We also estimate the variance of shocks to the non-growth component, σ_z^2, to be substantially higher. Closing the model with nominal yield curve dynamics, renders the real rate gap stationary and makes r_t^* track the real rate of interest more closely than in HLW as we will discuss below. Accordingly, the non-growth component needs to be able to capture a larger wedge between expected potential output growth and the trend in the natural real rate, thereby

requiring a larger innovation variance.

The coefficients of the VAR for slope and curvature support the stationarity assumption. The own lag coefficients, a_{11} and a_{22}, are at around 0.6 and the largest eigenvalue of the (sub-)VAR at the posterior median is around 0.86, substantially smaller than unity.

Finally, the estimated variance of measurement errors for yields, $\sigma_y(\tau)$, are almost all below 10 basis points, implying a fit of yields similar to benchmark term structure models (see, e.g., Diebold and Li, 2006), with the exception of maturities below one year. Also, the standard deviation of the measurement error corresponding to the inflation surveys, $\sigma^2_{s,\pi}$, is fairly tight hence keeping model-based long-run inflation expectations relatively close to their survey-based counterpart. A similar order of magnitude prevails for the measurement errors of the 1-year ahead short-term interest rate survey, with a standard deviation of 13 basis points. The latter is particularly helpful in informing the model about the high persistence of short-term rate at the effective lower bound (ELB), even if not modeled explicitly.

4 Quantitative results

This section presents the r^*_t estimates in Section 4.1, discusses which observables are important in the inference of r^*_t in Section 4.2, and reports the term premium estimates compared with results from stationary yield curve models in Section 4.3.

4.1 Estimates of the natural rate of interest, r^*_t

Figure 4.1 plots our posterior median estimate of the natural real interest rate together with its 90% credible set and compares it to estimates from Laubach and Williams (2016), denoted "LW", HLW, denoted "HLW", and Bauer and Rudebusch (2020), denoted "BR".[18] Hence, the figure provides an r^*_t comparison based on a macro (LW and HLW), a finance (BR) and a macro-finance (BGL) approach. Our r^*_t estimates appear closer to those by BR than those by HLW or LW.[19] We note the following results:

First, our estimates are lower than LW and HLW during the 1960s and 1970s and following the Global Financial Crisis. Rather than showing a continued decline over that period, our

[18] The BR estimate is based on the estimated-shifting-endpoint (ESE) approach and constructed by subtracting the authors' measure for long-run inflation expectations from their estimated i^*_t as shown in Figure 4 of their paper.

[19] The correlation of quarterly changes between our estimate and BR amounts to 0.39 versus 0.22 and 0.06 between our estimates and LW or HLW, respectively.

Figure 4.1: Comparison of r_t^* estimates

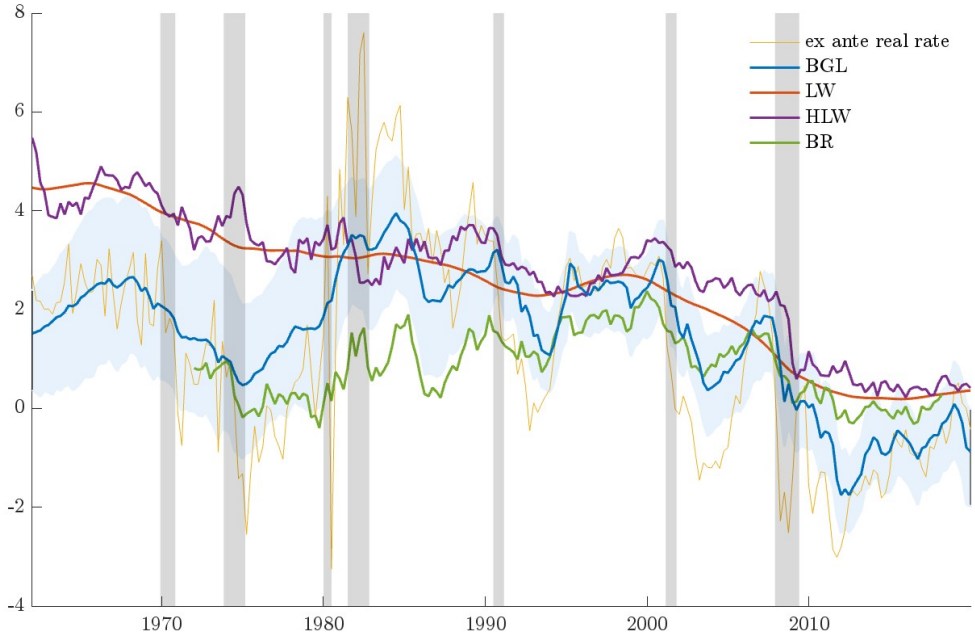

Note: The figure shows our (BGL) median r_t^* estimates together with its 90% credible set and compares it to estimates from LW, HLW and Bauer and Rudebusch (2020). The latter is calculated by subtracting the authors' measure of long-run inflation expectations from their i_t^* estimate. LW and HLW estimates are taken from the New York Fed website. NBER recessions are marked in grey.

estimates – as well as those of Bauer and Rudebusch (2020) when they become available in the early 1970s – exhibit a protracted rise and fall over the last six decades. Our estimates track real rates, as proxied here by the ex ante model-implied real rates, more closely. In our model, the actual real rate and its natural counterpart are co-integrated and their difference is stationary. Accordingly, the model-implied real rate gap

$$\tilde{r}_t = i_t - E_t\pi_{t+1} - r_t^* = \theta_S(1)(S_t - \bar{S}) + \theta_C(1)(C_t - \bar{C}) + \tilde{L}_t - E_t\tilde{\pi}_{t+1}, \tag{18}$$

is stationary and has mean zero. This stationarity is a key difference to HLW who treat the short-term real rate as an exogenous variable, not tying ex ante and natural real rate together, with the consequence that the real rate gap can be large and persistent, generating highly persistent output gaps. Compared to our model-implied ex ante real rate, the real rate gap of HLW persistently exceeds a magnitude of 300 basis points for almost the entire first two decades of our sample, as shown in Figure 4.2. Interpreting this gap as a measure of a monetary

policy stance implies a timing, extent, and duration of monetary easing that seems not perfectly plausible in light of inflation outcomes, notwithstanding the Great Inflation period which was also characterized by unprecedented commodity price shocks and a lose fiscal stance (Blinder, 1982). More to the point, the significantly stronger degree of policy accommodation measured by HLW during the post Global Financial Crisis decade seems difficult to reconcile with tepid inflation prints relative to target at the time.

Figure 4.2: Real rate gap $\tilde{r}_t$

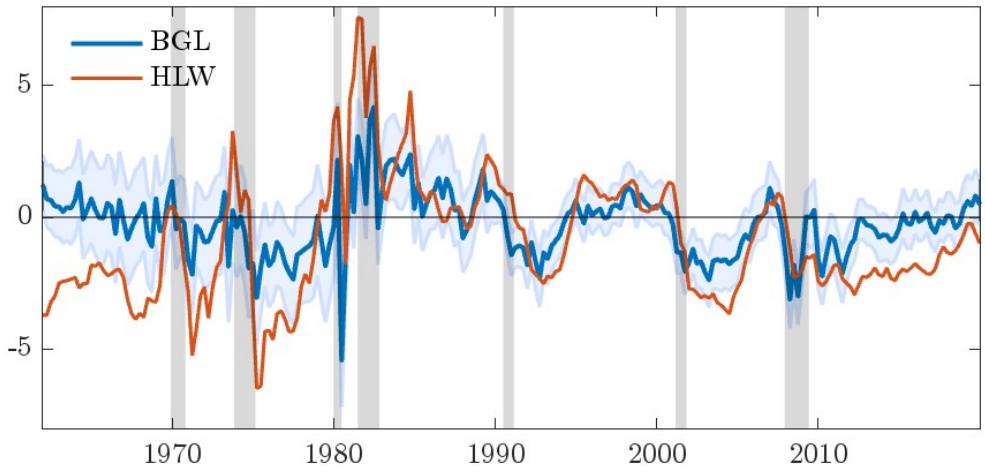

Note: The figure shows our (BGL) median $\tilde{r}_t$ estimate together with its 90% credible set and compares it to the real rate gap from HLW, calculated by subtracting their r_t^* estimate from their real rate measure. Both HLW series are downloaded from the New York Fed. NBER recessions are marked in grey.

Second, statistical uncertainty surrounding our estimates appears to be confined, with the average 95th-5th interpercentile range (IPR) equal to 2.3 percentage points (ppt) and notably less following the availability of short-term interest rate surveys as of 1990Q1 (2.9 ppt before 1990Q1, and 1.7 ppt thereafter, on average). This range compares rather favourably to the 8 ppt range identified for HLW estimates by Fiorentini et al. (2018).

Third, notwithstanding their different gauges of natural rate *levels*, all estimates agree on a decrease of r_t^* since the early 2000s, the extent of that decline ranging between two and three percentage points. Moreover, all models (excluding the very smooth estimates from Laubach and Williams, 2016) appear to decline during recessions and display a particularly strong drop in r_t^* following the GFC. We can even confirm the trend decline from a statistical perspective, taking the uncertainty about r_t^* estimates into account: the posterior density of the change in r_t^* between 2000 and end-2019 excludes zero from the associated 99% credible set. The same holds

true for the change since 2007Q2. For the time before 2000, only LW and HLW show a clear downward trend. To gauge the drivers of that decline, the left-hand side panel of Figure 4.3 provides the breakdown of r_t^* into its expected trend growth g_t and the catch-all, non-growth component z_t as outlined in Equation (3). While expected potential real growth has fluctuated around 3% per annum prior to the GFC, it fell to around 2% in the wake of the GFC, thereby partially contributing to the decline in r_t^*. However, the decline in the z-component is much larger. The non-growth component declined by about 2 percentage points in the wake of the GFC, possibly reflecting an increased demand for safe assets as reported by e.g. Del Negro et al. (2017).

Figure 4.3: Natural rate of interest and its components

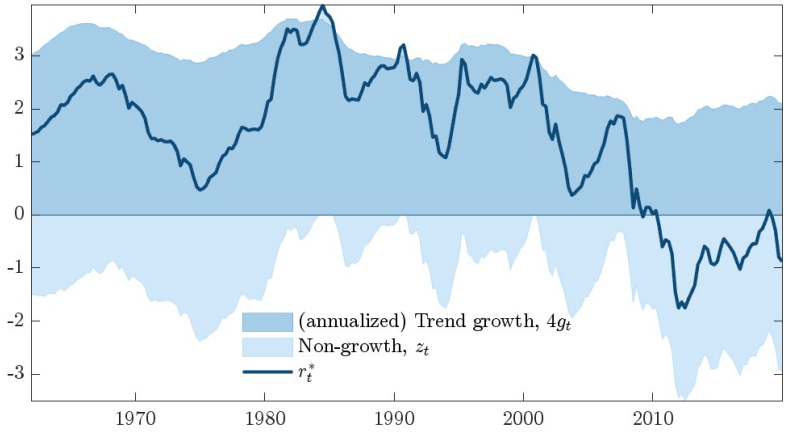

Note: The figure shows the decomposition of r_t^* into annualized expected trend growth $4g_t$ and the non-growth component z_t.

4.2 What data inform the inference on r_t^*?

Our model uses macro, yield curve and survey data to estimate r_t^*. To get an impression on the relevance of the different measurement data for the estimation of r_t^*, we apply the historical data decomposition of Koopman and Harvey (2003) to estimate the share of contributions from observed variables to latent factors. For the smoothed estimates of r_t^* and its components g_t and z_t Figure 4.4 shows the contribution from specific groups of observables on the respective estimate.[20]

[20]Recall that surveys on short-rate expectations over short horizons ("i surveys" in Figure 4.4) only enter our data set as of 1989Q2; however, these survey data points also matter for the *smoothed* estimates of r_t^* and other state variables before 1989Q2.

All three sources inform r_t^*: macro, yield curve and survey data. Unsurprisingly, the expected potential growth rate g_t (left panel) is primarily informed by log real GDP. Yet, for the non-growth component, z_t (middle panel) and hence r_t^* (right panel), yield curve and survey data play important roles in the inference as well. Specifically, the inference about r_t^* depends positively on interest rate data on net, and negatively on inflation and long-term inflation expectations in line with the calculation of an ex ante real rate.

One key feature is that neither the short- nor long-term rate *alone* is informative about r_t^* but the entire yield curve. This holds particularly for the ZLB period.

An alternative way to gauge the contribution of different observables to the estimation of r_t^* is to recover the latent states using only subsets of the data, taking as given the posterior estimated parameters (see Appendix F for details). The analysis confirms that all three data sources are relevant for inferring the level of r_t^*. Moreover, the version *without* financial data gives rise to mostly higher and significantly smoother r_t^* estimates throughout the first three decades of the sample. This result supports our conjecture that closing the model with an endogenous interest rate equation generates more cyclical r_t^* estimates and thereby less persistent real rate gap measures, especially in the first part of the sample.

Finally, exploiting the information of the entire yield curve also supports the identification of both the cyclical and stochastic trend components of real rates as discussed in more detail in Section 5.3, where we estimate the model using only the short-term rate.

Figure 4.4: Historical data decomposition of r_t^*

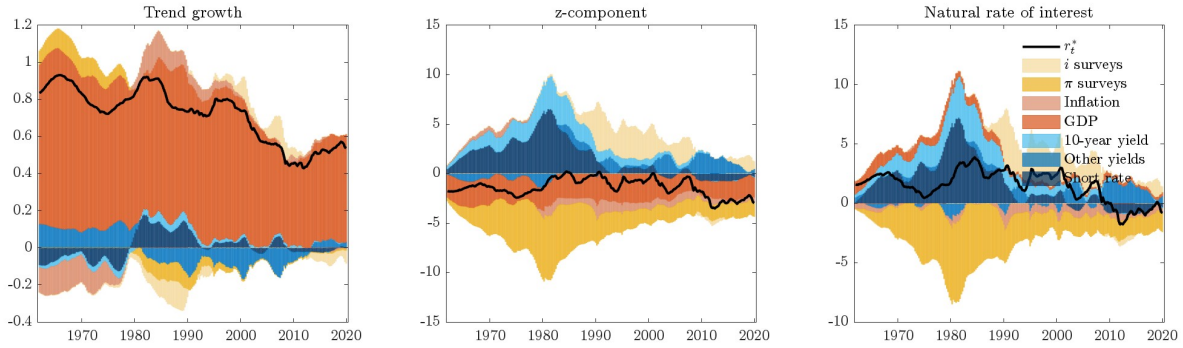

Note: The Figure shows the decomposition of selected latent states into the contributions of observables as inferred by the Kalman smoother, based on posterior median estimates. See Koopman and Harvey (2003) for details on how to compute the weights.

4.3 Term premia

Our term premia estimates from Equation (15) are affected by accounting for trends in r_t^* and π_t^*. On the left, Figure 4.5 shows our decomposition of the 5-year forward rate 5-years ahead into the expectations component (i.e. the average expected short-term interest rate over that 5-year horizon, 5-years ahead) and the forward term premium. A comparison with estimates commonly reported in the literature on the right of Figure 4.5 shows a high consistency in the dynamics.

Yet, while term-premia estimates from the literature display a distinct stochastic trend, especially for the long forward horizon, our term premia rather show cyclical dynamics.[21] Less trending and more cyclical term premia reflect the underlying model mechanics: while the standard modeling approach is based on stationary factor dynamics and a time-invariant long-run mean for the short rate, our model features a time-varying and non-stationary attractor for the short-term interest rate. Accordingly, the expectations component is able to absorb a relatively larger part of the trend in long-term bond yields in our model, and the term premium does not have to incorporate a trend as criticized by e.g. Cochrane (2007).[22]

Figure 4.5: 5-year-in-5-year forward term premium estimates

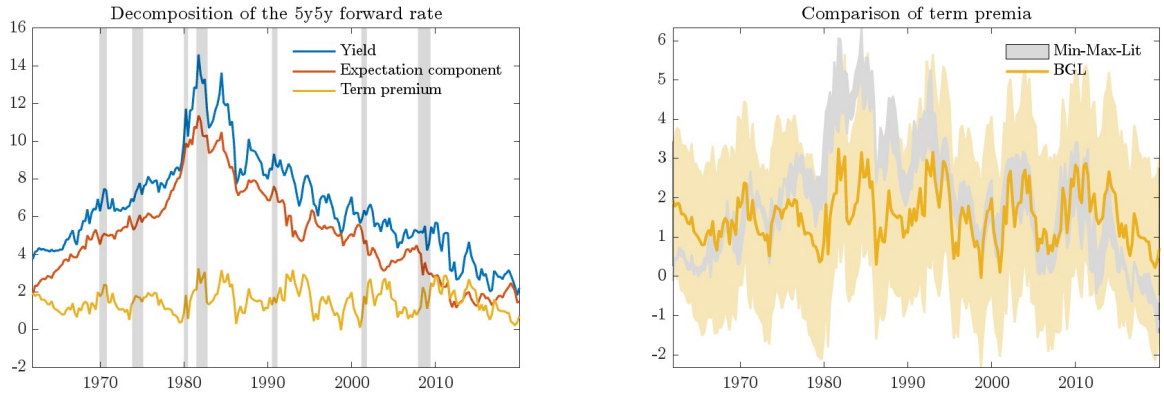

Note: The left figure shows the decomposition of the 5-year-in-5-year forward rate (blue) into the model-implied expectation component (red) and the term premium (yellow). The right figure compares our term premium estimate for the 5-year-in-5-year forward rate with a min-max-range (grey area) from several estimates in the literature: Kim and Wright (2005) (taken from FRED), Adrian et al. (2013) and a DNS model following Diebold and Li (2006), both based on authors' calculations.

A recent important exception to the dominance of stationary models is Bauer and Rudebusch

[21] Unless noted differently, we use the term "cyclical" in the sense of the time series not showing a distinct trend but rather "looking stationary", and not in the narrow sense of correlating with the business cycle.

[22] Abbritti et al. (2023) obtain similar term premium dynamics, in particular not exhibiting a clear trend, based on a fractional cointegration approach.

(2020) who also incorporate a trend for long-horizon short-rate expectations. Their term premia estimates (Figure 4.6) for long-horizon forwards are less trending than those from constant-mean models, but still somewhat less cyclical than our term premia. This "in-between" pattern could arise from our model specification enforcing stationary term premia by construction, as opposed to their approach.

Figure 4.6: Forward term premia: comparison with Bauer and Rudebusch (2020)

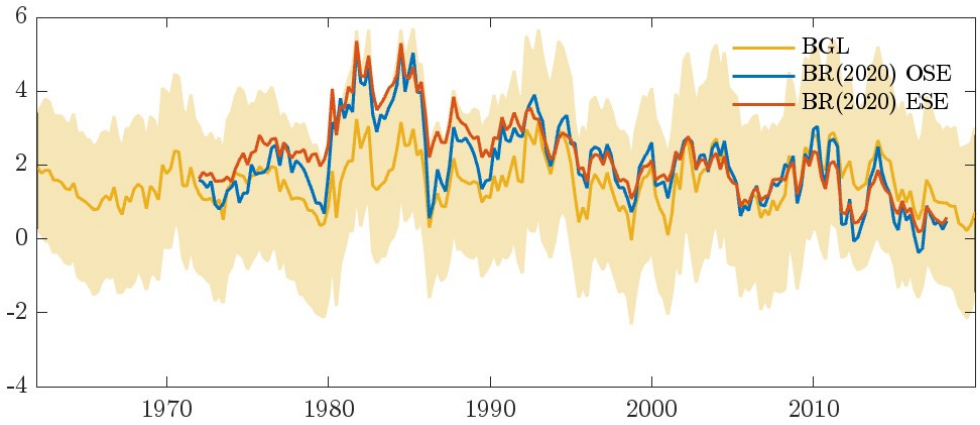

Note: The figure compares our (BGL) term premium estimate of the 5-year-in-5-year forward rate (in yellow) with those presented in Bauer and Rudebusch (2020). OSE (in blue) denotes the model with observed shifting endpoint, while ESE (in red) denotes the model with estimated shifting endpoint.

5 Model extensions

In this section, we discuss model extensions and robustness checks. We allow long-term (rather than short-term) real interest rates to enter the IS curve in Section 5.1 and specify a shadow rate term structure model to address the ELB in Section 5.2. Finally, we discuss additional robustness exercises in Section 5.3.

5.1 Different maturities of real rates

By adding yield curve dynamics to the baseline Laubach and Williams model, we can test their modeling assumption that only the short-term – rather than the longer-term – real rate gap drives the output gap in Equation (J.34). Doing so brings the model closer to structural New Keynesian models in which the expected path of future short-term real interest rates determines households' consumption decisions and ultimately output.

Specifically, we assume that the IS curve takes the form:

$$\begin{aligned}\tilde{x}_t &= a_1\tilde{x}_{t-1} + a_2\tilde{x}_{t-2} \\ &\quad + a_3 E_{t-1}\sum_{l=1}^{2}\left[y_{t-l}(\tau) - \frac{1}{\tau}\sum_{j=1}^{\tau}\pi_{t-l+j} - \left(y^*_{t-l}(\tau) - \frac{1}{\tau}\sum_{j=1}^{\tau}\pi^*_{t-l+j}\right)\right] + \varepsilon^{\tilde{x}}_t. \qquad (19)\end{aligned}$$

The term in square brackets represents the average (lagged) long-term real rate gap for maturity τ. We measure long-term real rates by subtracting average expected inflation over the next τ years from the corresponding nominal bond yield $y(\tau)$. The second pair of terms (in parentheses) is the natural counterpart to this real rate. As in our baseline specification with one-period real rate gaps, in turn following HLW, we take the average of the $t-1$ and $t-2$ long-term real rate gap.

In doing so, we make two assumptions. First, while we subtract inflation expectations to deflate nominal interest rates into real rates, we ignore the cyclical component of inflation risk premia, because our nominal pricing model is mute on the separation of nominal term premia into inflation risk and real rate risk compensation.[23] Second, we use the $t-1$ information set for the conditional expectations for both lags as lagged expectations themselves become a state variable, thereby substantially increasing the state space and the computational challenges for solving the model.

Even under these slightly simplifying assumptions, the IS equation (19) with a long-term real rate gap of maturity τ requires the computation of model-consistent inflation expectations over τ horizons. Expected inflation in period $t+\tau$, however, is a function of the expected output gap and inflation in periods $t+\tau-1$. The former, in turn, depends on $t+\tau-1$ real rate gaps and hence inflation expectations. Appendix H documents the required solution to this dynamic programming problem.

Table 5.1 presents the results of a model comparison exercise with respect to the maturity of the real rate gap. The data prefer model specifications that include longer-term real rate gaps, with the highest marginal likelihood being reached at the 10-year horizon.[24]

[23] Aruoba (2020), Brzoza-Brzezina and Kotłowski (2014), Imakubo et al. (2018) and Dufrénot et al. (2022) also construct real yield data by subtracting proxies of inflation expectations from the nominal yield curve, i.e. without factoring in inflation risk premia. Also economically, it may not be too far fetched to assume that firms and consumers observe nominal rates and just subtract inflation expectations to arrive at a real measure that informs their consumption and production/investment decisions. Finally, Appendix H contains a comparison with real rates of inflation-linked bonds, which display a distinct co-movement with our measure.

[24] Going beyond 10-year rates in this exercise would require extending the cross section of yield data. However, we stick to the 10-year rate as maximum, noting it is a prominent maturity in related exercises, see, e.g. Kiley

Table 5.1: Marginal data densities for models with different real rate gaps

Maturity τ (in quarter)	1	4	8	20	28	32	40
Marginal likelihood	-1859.6	-1892.5	-1986.0	-1847.0	-1776.5	-1764.2	-1742.0

Note: The first row contain the maturity of the long-term real rate used in the IS equation, see (19). The marginal likelihood is based on the harmonic mean estimator proposed by Gelfand and Dey (1994) and based on a single chain with 100,000 iterations, of which the first 90,000 were burn-in and afterwards every 10th draw was retained.

Yet differences in maturities of the real rate gap do not impact latent variable estimates. In particular, the left-hand panel of Figure 5.1 shows that the posterior median estimates of r_t^* estimates are little, if at all, affected. An explanation for this result could be that the level factor is the most prominent source of variation in yields across maturities. Thus, for any maturity τ, the cyclical level factor is a key driver of the corresponding real rate gap. Having learned about the cyclical level factor $\tilde{L}$ from any real-rate gap specification with maturity τ in a similar way, having inferred the overall level factor L_t from yield curve dynamics, and noting that π^* closely follows survey information, it follows that the different specifications imply similar levels of r_t^* given that $r_t^* = L_t - \pi_t^* - \tilde{L}_t$,

Real rate gaps based on longer-term yields generate overall narrower uncertainty bands, in particular since 1990Q1 (right panel of Figure 5.1). This result supports the findings in Table 5.1 that the use of long-term real rate gaps in the IS curve is preferred by the data.

Figure 5.1: The effect of different real rate horizons on r_t^* (see Table 5.1) and its uncertainty

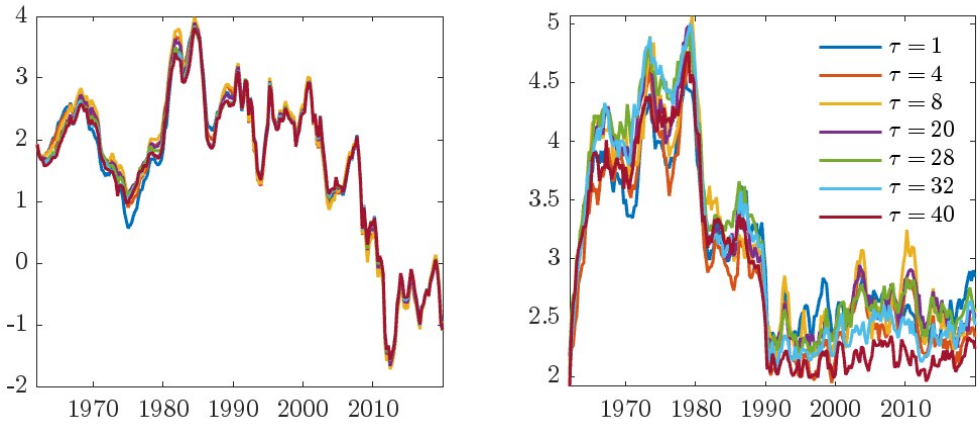

Note: Left-hand side panel shows posterior median estimates of r_t^* of the different model specifications. Right-hand side panel shows the 95th-5th interpercentile range of r_t^*.

While our semi-structural macro-finance model highlights the relevance of longer-term rates

(2014), Fuhrer and Rudebusch (2004), or Brayton et al. (2014).

in the IS Curve, it does not allow for a deeper economic interpretation of why long maturities are preferred. Future research may explore this in a structural framework.

5.2 Accounting for the effective lower bound (ELB)

During the last decade of our sample, the short-term interest rate was constrained by the ELB. Ignoring this constraint may affect our estimates of r_t^*. We therefore extend our macro-finance model to a shadow-rate model by imposing a lower bound on interest rates. Following Feunou et al. (2022), we approximate the ELB constraint using the following smooth nonlinear function:

$$i_t = \theta\omega\left(\frac{s_t}{\theta}\right), \tag{20}$$

where $i_t \equiv y_t(1)$, $\omega(x) = x\Phi(x) + \phi(x)$ and Φ and ϕ denote the cumulative distribution and probability density function of a standard normal distribution, respectively.[25] The function ensures that $i > 0$ for all levels of the shadow rate s, but the mapping varies with θ. The function resembles a "hockey stick" exhibiting a more distinct kink for θ closer to zero. For sufficiently positive shadow rates (large enough $x > 0$), we have $\omega(x) \approx x$ and the set-up converges to a linear model.

This approach provides for a tractable and "almost arbitrage-free" pricing of bonds[26] but the resulting state space model becomes nonlinear. We use the extended Kalman filter for estimation and leave details on the model and estimation to the Appendix I.

The shadow-rate specification passes the consistency check that bond yields behave very similarly to those in our linear baseline model when the state vector implies that the short rate is sufficiently positive. The resulting estimate of the shadow rate is shown in the left panel of Figure 5.2 over the period 2008-2019. The shadow rate falls below zero in 2009Q1, reaches its lowest point -2% in 2014Q2, and remains in negative territory until 2015Q4, just before the completion of active asset purchases. Our estimated shadow rate displays similar dynamics to that of Wu and Xia (2016), yet the through is less negative than their estimate and uncertainty is sizeable.

The right-hand panel of Figure 5.2 compares the r_t^* estimate of the baseline and the ELB versions of the model. The estimates of r_t^* from the shadow-rate model are somewhat more

[25] Opschoor and van der Wel (2025) also deploy this specification for the mapping from shadow rate to short rate (among other functional forms).

[26] See Feunou et al. (2022) for the exact notion.

Figure 5.2: Model-implied shadow rate (left) and r_t^* comparison (right)

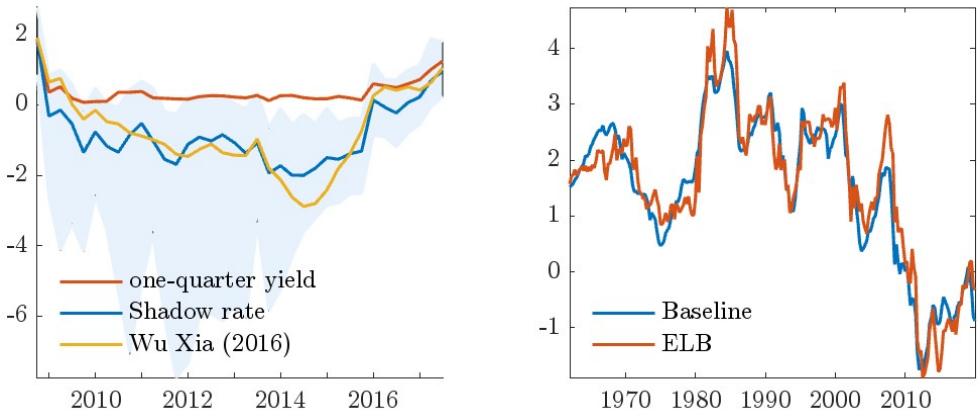

Note: The left panel shows the observed one-quarter rate together with the model-implied shadow rate and the shadow rate from Wu and Xia (2016) from 2008Q3 until 2017Q2. The shaded area represents the 90% credible set. The right panel compares the r_t^* estimates of the baseline model without ELB (blue) to the shadow rate model (red).

volatile, which probably owes to the nonlinear estimation approach. Taking estimation uncertainty into account, the figure does not suggest an economically meaningful difference between the two estimates.

5.3 Other robustness exercises

In this section, we briefly discuss the robustness of our main results with respect to the sample length and some modeling choices. Further details are relegated to our Appendix, Section J.

First, latent factor estimates are robust to different subsample choices, as highlighted by a pseudo-real-time analysis. The analysis also indicates that even for shorter samples estimation uncertainty surrounding r_t^* is confined in our setup.

Second, as discussed in Section 4.1, the model by LW and HLW is not "closed" as it treats the actual short-term real rate as exogenous. While in the main part of the paper, short-term interest rate dynamics are specified as part of the full yield curve evolution, we check robustness with respect to the simplest alternative which decomposes the short-term nominal interest rate into a stochastic trend and a stationary cyclical component. As we show in the Appendix, despite a tighter prior of the lagged inflation gap in the Phillips curve, the resulting posterior estimates of r_t^* are more volatile. Also, estimation uncertainty is substantially higher in the first half of the sample.

Third, we generalize the arbitrage-free term structure module by not imposing the specific

Dynamic Nelson Siegel parameterization which is a constrained version of the canonical form of Joslin et al. (2011a).[27] The more flexible specification improves the model fit somewhat but leaves the estimated latent states and other results unaffected.

Fourth, we extend the model to allow for stochastic volatility in the IS and Phillips curve. The cyclical dynamics pinned down by both structural equations (J.34) and (4) are key determinants of r_t^* whose identification might be comprised by instability of the disturbance variances over time. The implementation follows Jacquier et al. (1994) and adds a sequential independence Metropolis Hastings step to our Gibbs sampler. While both posterior median volatility series show sizable time variation, the effect on the posterior estimates of latent states and parameters is negligible.

Fifth, our baseline model postulates a very parsimonious structure for the cyclical level factor dynamics. Generalizing the model by assuming that the stationary yield curve factors $(\tilde{L}_t, S_t, C_t)$ jointly follow a trivariate VAR – with the output and inflation gap as exogenous variables – does not affect the results.

Sixth, our baseline model assumes a relatively tight prior on the variance of trend growth to ensure smooth dynamics in the growth of potential output. We show that a less tight prior causes our estimate for trend growth g_t to soak up some of the cyclical dynamics in output, thus rendering the resulting output gap less persistent. The non-growth component, however, adjusts accordingly leaving our estimates for r_t^* virtually unaffected.

Seventh, in light of the weak empirical relationship between real rates and growth documented in Lunsford and West (2019), we relax the assumption that the expected annualized trend growth rate, g_t, loads one-to-one into r_t^*, i.e. with a fixed coefficient of 4 in (3). Instead, we estimated the loading coefficient using a flat prior centered around 4. While the posterior median turns out to be lower than the value imposed by Laubach and Williams (2003, 2016), we find a significantly positive effect of expected real potential growth on trend real interest rates with a posterior median estimate of the coefficient at 2.74, and the 90% credible set ranging from 1.4 to 4.4. This finding is in line with standard theory that links real rates to per-capita consumption growth.

Finally, we relax the assumption of the original Laubach and Williams model that both lags of the real rate gap in the IS curve (J.34) affect the output gap in the same way by estimating a model version with separate coefficients for each lag. However, the posterior distributions for

[27] See the supplement of Joslin et al. (2011a).

both parameters largely overlap and the difference is not statistically significant. Relaxing this constraint therefore only adds estimation uncertainty while leaving the r_t^* estimates unaffected.

6 Conclusion

In this paper, we propose a novel macro-finance model with the natural real rate of interest fulfilling a dual role. For the yield curve, r_t^*, together with trend inflation π^*, constitutes a time-varying anchor. For the real economy, r_t^* indicates the real rate of interest consistent with the economy operating at its potential level. Our r_t^* estimates balance both roles. Nominal term premia implied by the model are consistent with the time variation in r_t^*. We therefore address the "natural rate puzzle" as recently claimed by Davis et al. (2024), who criticize the existing literature that tends to use macro and finance information rather separately and inconsistently to obtain estimates of r_t^* and bond risk premia.

Despite using the same semi-structural macroeconomic relations as in LW and HLW, our r_t^* estimates imply a real rate gap (actual real rate minus r_t^*) that is distinctly cyclical, contrasting with the highly persistent estimates of their paper. This difference arises because our stipulated yield curve model endogenizes the real rate and renders the real rate gap stationary, while the real rate in HLW is exogeneous and the real rate gap can vary arbitrarily.

Our macro-finance model is estimated by Bayesian methods (rather than by multi-step ad-hoc approaches as frequently encountered in the literature) which allows for consistent inference about the uncertainty surrounding parameters and latent states. The set-up also allows for specification analysis regarding the question of whether longer-maturity rate gaps are more adequate drivers of the output gap than the standard short-term real rate gaps. We find evidence favoring the inclusion of longer-term yields.

Future research may expand the model by including explicitly a term structure of both nominal and inflation-linked bonds, or by enriching the specification to account for central bank asset purchases in the spirit of Li and Wei (2013).

References

Abbritti, M., Carcel, H., Gil-Alana, L., and Moreno, A. (2023). Term premium in a fractionally cointegrated yield curve. *Journal of Banking & Finance*, 149(106777).

Adrian, T., Crump, R. K., and Moench, E. (2013). Pricing the term structure with linear regressions. *Journal of Financial Economics*, 110(1):110–138.

Ajevskis, V. (2020). The natural rate of interest: information derived from a shadow rate model. *Applied Economics*, 52(47):5129–5138.

Aruoba, S. B. (2020). Term structures of inflation expectations and real interest rates. *Journal of Business & Economic Statistics*, 38(3):542–553.

Aruoba, S. B. and Schorfheide, F. (2011). Sticky prices versus monetary frictions: An estimation of policy trade-offs. *American Economic Journal: Macroeconomics*, 3(1):60–90.

Bauer, M. D. and Rudebusch, G. D. (2020). Interest rates under falling stars. *American Economic Review*, 110(5):1316–54.

Blinder, A. S. (1982). The anatomy of double-digit inflation in the 1970s. In Hall, R. E., editor, *Inflation: Causes and effects*, pages 261–282. Chicago: University of Chicago Press.

Brand, C., Bielecki, M., and Penalver, A. (2018). The natural rate of interest: Estimates, drivers, and challenges to monetary policy. ECB Occasional Paper 217, European Central Bank.

Brand, C. and Mazelis, F. (2019). Taylor-rule consistent estimates of the natural rate of interest. ECB Working Paper 2257, European Central Bank.

Brayton, F., Laubach, T., and Reifschneider, D. (2014). Optimal-control monetary policy in the FRB/US model. *FEDS notes*.

Brzoza-Brzezina, M. and Kotłowski, J. (2014). Measuring the natural yield curve. *Applied Economics*, 46(17):2052–2065.

Buncic, D. (2024). Econometric issues in the estimation of the natural rate of interest. *Economic Modelling*, 132:106641.

Caballero, R. J., Farhi, E., and Gourinchas, P.-O. (2017). Rents, technical change, and risk premia accounting for secular trends in interest rates, returns on capital, earning yields, and factor shares. *American Economic Review*, 107(5):614–20.

Carter, C. K. and Kohn, R. (1994). On Gibbs sampling for state space models. *Biometrika*, 81(3):541–553.

Carvalho, C., Ferrero, A., Mazin, F., and Nechio, F. (2025). Demographics and real interest rates across countries and over time. *Journal of International Economics*, 157(104127).

Christensen, J. H. and Mouabbi, S. (2024). The natural rate of interest in the euro area: evidence from inflation-indexed bonds. Federal Reserve Bank of San Francisco Working Paper 2024-08, Federal Reserve Bank of San Francisco.

Christensen, J. H. and Rudebusch, G. D. (2019). A new normal for interest rates? Evidence from inflation-indexed debt. *Review of Economics and Statistics*, 101(5):933–949.

Christensen, J. H. E., Diebold, F. X., and Rudebusch, G. D. (2011). The affine arbitrage-free class of Nelson–Siegel term structure models. *Journal of Econometrics*, 164:4–20.

Cieslak, A. and Povala, P. (2015). Expected returns in treasury bonds. *The Review of Financial Studies*, 28(10):2859–2901.

Cochrane, J. H. (2007). Commentary on "Macroeconomic implications of changes in the term premium". *Federal Reserve Bank of St. Louis Review*, 89(4):271–282.

Cogley, T. and Sargent, T. J. (2005). Drifts and volatilities: monetary policies and outcomes in the post WWII US. *Review of Economic Dynamics*, 8(2):262–302.

Davis, J., Fuenzalida, C., Huetsch, L., Mills, B., and Taylor, A. M. (2024). Global natural rates in the long run: Postwar macro trends and the market-implied r* in 10 advanced economies. *Journal of International Economics*, 149. Article No. 103919.

Del Negro, M., Giannone, D., Giannoni, M. P., and Tambalotti, A. (2017). Safety, liquidity, and the natural rate of interest. *Brookings Papers on Economic Activity*, 2017(1):235–316.

Del Negro, M., Giannoni, M. P., and Schorfheide, F. (2015). Inflation in the great recession and New Keynesian models. *American Economic Journal: Macroeconomics*, 7(1):168–196.

Dewachter, H., Iania, L., and Lyrio, M. (2014). Information in the yield curve: A macro-finance approach. *Journal of Applied Econometrics*, 29(1):42–64.

Diebold, F. X. and Li, C. (2006). Forecasting the term structure of government bond yields. *Journal of Econometrics*, 130(2):337–364.

Dufrénot, G., Rhouzlane, M., and Vaccaro-Grange, E. (2022). Potential growth and natural yield curve in Japan. *Journal of International Money and Finance*, 124(102628).

Durbin, J. and Koopman, S. J. (2002). A simple and efficient simulation smoother for state space time series analysis. *Biometrika*, 89(3):603–616.

Durbin, J. and Koopman, S. J. (2012). *Time Series Analysis by State Space Methods*. Oxford University Press, 2nd edition.

Feunou, B. and Fontaine, J.-S. (2021). Secular economic changes and bond yields. *The Review of Economics and Statistics*, 105(2):408–424.

Feunou, B., Fontaine, J.-S., Le, A., and Lundblad, C. (2022). Tractable term structure models. *Management Science*, 68(11):8411–8429.

Fiorentini, G., Galesi, A., Pérez-Quirós, G., and Sentana, E. (2018). The rise and fall of the natural interest rate. Discussion Paper 13042, CEPR.

Fuhrer, J. C. and Rudebusch, G. D. (2004). Estimating the Euler equation for output. *Journal of Monetary Economics*, 51(6):1133–1153.

Geiger, F. and Schupp, F. (2018). With a little help from my friends: survey-based derivation of euro area short rate expectations at the effective lower bound. Discussion Paper 27/2018, Deutsche Bundesbank.

Gelfand, A. E. and Dey, D. K. (1994). Bayesian model choice: asymptotics and exact calculations. *Journal of the Royal Statistical Society: Series B (Methodological)*, 56(3):501–514.

Geweke, J. F. (1991). Evaluating the accuracy of sampling-based approaches to the calculation of posterior moments. Staff Working Paper 148, Federal Reserve Bank of Minneapolis.

González-Astudillo, M. and Laforte, J.-P. (2025). Estimates of the natural rate of interest consistent with a supply-side structure and a monetary policy rule for the us economy. *International Journal of Central Banking*, 21(1):137–199.

Gourinchas, P.-O. and Rey, H. (2019). Global real rates: a secular approach. BIS Working Paper Series 793, Bank for International Settlements.

Gürkaynak, R. S., Sack, B., and Wright, J. H. (2007). The US Treasury yield curve: 1961 to the present. *Journal of Monetary Economics*, 54(8):2291–2304.

Gürkaynak, R. S., Sack, B., and Wright, J. H. (2010). The TIPS yield curve and inflation compensation. *American Economic Journal: Macroeconomics*, 2(1):70–92.

Holston, K., Laubach, T., and Williams, J. C. (2017). Measuring the natural rate of interest: international trends and determinants. *Journal of International Economics*, 108:S59–S75.

Imakubo, K., Kojima, H., and Nakajima, J. (2018). The natural yield curve: its concept and measurement. *Empirical Economics*, 55(2):551–572.

Jacquier, E., Polson, N. G., and Rossi, P. E. (1994). Bayesian analysis of stochastic volatility models. *Journal of Business & Economic Statistics*, 12(4):371–389.

Johannsen, B. K. and Mertens, E. (2021). A time-series model of interest rates with the effective lower bound. *Journal of Money, Credit and Banking*, 53(5):1005–1046.

Joslin, S., Singleton, K. J., and Zhu, H. (2011a). A new perspective on Gaussian dynamic term structure models. *The Review of Financial Studies*, 24(3):926–970.

Joslin, S., Singleton, K. J., and Zhu, H. (2011b). Supplement to "a new perspective on Gaussian dynamic term structure models". *The Review of Financial Studies*, 24(3):926–970.

Kiley, M. T. (2014). The aggregate demand effects of short- and long-term interest rates. *International Journal of Central Banking*, 10(4):69–104.

Kim, C.-J. and Kim, J. (2013). The pile-up problem in trend-cycle decomposition of real GDP: Classical and Bayesian perspectives. Technical report, Ludwig Maximilians Universität München.

Kim, D. H. and Wright, J. H. (2005). An arbitrage-free three-factor term structure model and the recent behavior of long-term yields and distant-horizon forward rates. FEDS Working Paper 2005-33, Federal Reserve Board.

Koopman, S. J. and Harvey, A. (2003). Computing observation weights for signal extraction and filtering. *Journal of Economic Dynamics and Control*, 27(7):1317–1333.

Kopp, E. and Williams, P. D. (2018). A macroeconomic approach to the term premium. IMF Working Paper 18/140, International Monetary Fund.

Kozicki, S. and Tinsley, P. A. (2001). Shifting endpoints in the term structure of interest rates. *Journal of Monetary Economics*, 47(3):613–652.

Laubach, T. and Williams, J. C. (2003). Measuring the natural rate of interest. *Review of Economics and Statistics*, 85(4):1063–1070.

Laubach, T. and Williams, J. C. (2016). Measuring the natural rate of interest redux. *Business Economics*, 51(2):57–67.

Li, C., Niu, L., and Zeng, G. (2012). A generalized arbitrage-free Nelson-Siegel term structure model with macroeconomic fundamentals. mimeo, SSRN.

Li, C. and Wei, M. (2013). Term structure modeling with supply factors and the Federal Reserve's large-scale asset purchase programs. *International Journal of Central Banking*, 9(1):3–39.

Lunsford, K. G. and West, K. D. (2019). Some evidence on secular drivers of US safe real rates. *American Economic Journal: Macroeconomics*, 11(4):113–139.

Mertens, E. (2016). Measuring the level and uncertainty of trend inflation. *Review of Economics and Statistics*, 98(5):950–967.

Mertens, E. and Nason, J. M. (2020). Inflation and professional forecast dynamics: An evaluation of stickiness, persistence, and volatility. *Quantitative Economics*, 11(4):1485–1520.

Mian, A. R., Straub, L., and Sufi, A. (2020). The saving glut of the rich. NBER Working Paper 26941, National Bureau of Economic Research.

Nelson, C. R. and Siegel, A. F. (1987). Parsimonious modeling of yield curves. *Journal of Business*, 60:473–489.

Opschoor, D. and van der Wel, M. (2025). A smooth shadow-rate dynamic nelson-siegel model for yields at the zero lower bound. *Journal of Business & Economic Statistics*, 43(2):298–311.

Papetti, A. (2019). Demographics and the natural real interest rate: historical and projected paths for the euro area. ECB Working Paper 2258, European Central Bank.

Rachel, Ł. and Summers, L. H. (2019). On secular stagnation in the industrialized world. *Brookings Papers on Economic Activity*, Spring 2019.

Stock, J. H. and Watson, M. W. (1998). Median unbiased estimation of coefficient variance in a time-varying parameter model. *Journal of the American Statistical Association*, 93(441):349–358.

Stock, J. H. and Watson, M. W. (2007). Why has US inflation become harder to forecast? *Journal of Money, Credit and Banking*, 39:3–33.

Taylor, J. B. (1993). Discretion versus policy rules in practice. In *Carnegie-Rochester conference series on public policy*, volume 39, pages 195–214. Elsevier.

Wu, J. C. and Xia, F. D. (2016). Measuring the macroeconomic impact of monetary policy at the zero lower bound. *Journal of Money, Credit and Banking*, 48(2-3):253–291.

Zaman, S. (2024). A unified framework to estimate macroeconomic stars. Federal Reserve Bank of Cleveland Working Paper Series 21-23R, Federal Reserve Bank of Cleveland.

Appendix

A Baseline model

A.1 The state space representation

State equation: To write the model in state-space representation, let the $N \times 1$ state vector ξ_t comprise the term structure factors (cyclical level component, slope and curvature), trend inflation, potential output, expected potential output growth, the non-growth component of the natural rate, the cyclical component of inflation, the output gap and some lagged variables (to cater for the dynamic structure of our model):

$$\xi_t = \begin{pmatrix} \tilde{L}_t & S_t & C_t & \pi_t^* & x_t^* & g_t & z_t & \tilde{\pi}_t & \tilde{x}_t & \tilde{L}_{t-1} & S_{t-1} & C_{t-1} & \tilde{\pi}_{t-1} & \tilde{x}_{t-1} \end{pmatrix}'.$$

Before we summarize all model equations in state space form, we need to solve the model-consistent inflation expectations that enter the IS curve (1) through the real interest rate gap. To do so, start by calculating the real rate, $r_t = y_t(1) - E_t\pi_{t+1}$. Taking conditional expectations of inflation gives

$$E_t\pi_{t+1} = E_t\left[\pi_{t+1}^* + \tilde{\pi}_{t+1}\right] = \pi_t^* + b_1\tilde{\pi}_t + b_2\tilde{x}_t,$$

where the latter equality uses the Phillips curve, equation (4) in the main text. Substitution yields

$$r_t = y_t(1) - \pi_t^* - b_1\tilde{\pi}_t - b_2\tilde{x}_t.$$

Using equation (5) of the main text and $\mathcal{A}(1) = -\theta_s(1)\bar{S} - \theta_c(1)\bar{C}$, the real rate gap, $\tilde{r}_t = r_t - r_t^*$, is given by

$$\begin{aligned} \tilde{r}_t =& y_t(1) - \pi_t^* - b_1\tilde{\pi}_t - b_2\tilde{x}_t - r_t^* \\ =& \tilde{L}_t + \theta_s(1)(S_t - \bar{S}) + \theta_c(1)(C_t - \bar{C}) - b_1\tilde{\pi}_t - b_2\tilde{x}_t, \end{aligned}$$

where $\bar{S}$ and $\bar{C}$ denote the unconditional mean of slope and curvature, respectively. Using the fact that both the inflation gap $\tilde{\pi}_t$ and output gap $\tilde{y}_t$ are mean-zero by construction, both are given by

$$\begin{pmatrix} \bar{S} \\ \bar{C} \end{pmatrix} = \left(\mathbf{I_2} - \begin{pmatrix} a_{11} & a_{12} \\ a_{21} & a_{22} \end{pmatrix} \right)^{-1} \begin{pmatrix} a_{10} \\ a_{20} \end{pmatrix}.$$

Finally, substituting the equation for the real rate gap into the IS curve, yields the final state transition equation for the output gap:

$$
\begin{aligned}
\tilde{x}_t =& a_1\tilde{x}_{t-1} + a_2\tilde{x}_{t-2} + a_3\big(\tilde{r}_{t-1} + \tilde{r}_{t-2}\big) + \varepsilon_t^{\tilde{x}} \\
=& a_1\tilde{x}_{t-1} + a_2\tilde{x}_{t-2} + a_3\big(\tilde{L}_{t-1} + \theta_s(1)(S_{t-1} - \bar{S}) + \theta_c(1)(C_{t-1} - \bar{C}) - b_1\tilde{\pi}_{t-1} - b_2\tilde{x}_{t-1}\big) \\
&+ a_3\big(\tilde{L}_{t-2} + \theta_s(1)(S_{t-2} - \bar{S}) + \theta_c(1)(C_{t-2} - \bar{C}) - b_1\tilde{\pi}_{t-2} - b_2\tilde{x}_{t-2}\big) + \varepsilon_t^{\tilde{x}} \\
=& \big(a_1 - a_3b_2\big)\tilde{x}_{t-1} + \big(a_2 - a_3b_2\big)\tilde{x}_{t-2} \\
&+ a_3\big(\tilde{L}_{t-1} + \theta_s(1)(S_{t-1} - \bar{S}) + \theta_c(1)(C_{t-1} - \bar{C}) - b_1\tilde{\pi}_{t-1}\big) \\
&+ a_3\big(\tilde{L}_{t-2} + \theta_s(1)(S_{t-2} - \bar{S}) + \theta_c(1)(C_{t-2} - \bar{C}) - b_1\tilde{\pi}_{t-2}\big) + \varepsilon_t^{\tilde{x}}
\end{aligned}
$$

Combining this equation and the laws of motions for the other latent variables (2)–(4) and (11)–(13) in the main text, we can write the state equation compactly as:

$$\xi_t = \boldsymbol{\mu} + \mathbf{F}\xi_{t-1} + \mathbf{G}e_t, \quad e_t \sim \mathcal{N}(0, \mathbf{I}). \tag{A.1}$$

The vector of constant terms, $\boldsymbol{\mu}$ and the matrix $\mathbf{F}$ are given by:

$$\boldsymbol{\mu} = \begin{pmatrix} 0 & a_{10} & a_{20} & 0 & 0 & 0 & 0 & 0 & -a_3[\theta_s(1)\bar{S} + \theta_c(1)\bar{C}] & 0 & 0 & 0 & 0 & 0 \end{pmatrix}',$$

and

$$\mathbf{F} = \begin{pmatrix}
a_L & 0 & 0 & 0 & 0 & 0 & 0 & 0 & 0 & & & & & \\
0 & a_{11} & a_{12} & 0 & 0 & 0 & 0 & a_{13} & a_{14} & & \mathbf{0_{3\times5}} & & & \\
0 & a_{21} & a_{22} & 0 & 0 & 0 & 0 & a_{23} & a_{24} & & & & & \\
 & & & 1 & 0 & 0 & 0 & & & & & & & \\
 & \mathbf{0_{4\times3}} & & 0 & 1 & 1 & 0 & & & & & \mathbf{0_{4\times7}} & & \\
 & & & 0 & 0 & 1 & 0 & & & & & & & \\
 & & & 0 & 0 & 0 & 1 & & & & & & & \\
0 & 0 & 0 & 0 & 0 & 0 & 0 & b_1 & b_2 & 0 & 0 & 0 & 0 & 0 \\
a_3 & a_3\theta_s(1) & a_3\theta_c(1) & 0 & 0 & 0 & 0 & -a_3b_1 & a_1 - a_3b_2 & a_3 & a_3\theta_s(1) & a_3\theta_c(1) & -a_3b_1 & a_2 - a_3b_2 \\
 & \mathbf{I_{3\times3}} & & & & & & & & & \mathbf{0_{3\times11}} & & & \\
 & & & \mathbf{0_{2\times7}} & & & & \mathbf{I_{2\times2}} & & & & \mathbf{0_{2\times5}} & &
\end{pmatrix},$$

respectively. The matrix $\mathbf{G}$ is assumed to be diagonal with standard deviations of state innovations on the main diagonal.

Measurement equation: For the measurement variables, we assume that (log) real output and (year-on-year) inflation are measured without error so that both are simply the sum of their respective trend and cyclical component:

$$x_t = x_t^* + \tilde{x}_t \tag{A.2}$$

$$\pi_t = \pi_t^* + \tilde{\pi}_t \tag{A.3}$$

We further include as measurement a set of K zero-coupon bond yields of maturities ranging from τ_1=1 quarter to $\tau_K = 40$ quarters. We assume that the one-quarter short-term rate $i_t \equiv y_t(1)$ is matched without error, i.e. $\sigma^2(1) = 0$. All other observed yields $y_t(\tau_i)$ equal their model-implied counterpart in equation (5) of the main text plus a measurement error

$$y_t(\tau_i) = \mathcal{A}(\tau_i) + \tilde{L}_t + L_t^* + \theta_s(\tau_i)S_t + \theta_c(\tau_i)C_t + u_t^{\tau_i}, \quad u_t^{\tau_i} \sim \mathcal{N}(0, \sigma_{\tau_i}^2), \quad i = 1, \ldots, K. \tag{A.4}$$

Surveys are mapped into their model counterparts as described by equations (16)–(17) in the main text.

Our vector of measurements, ζ_t, thus collects the observed yields, output, inflation and surveys

$$\zeta_t = \Big(y_t(\tau_1), \quad \ldots \quad y_t(\tau_K), \quad x_t, \quad \pi_t, \quad E_t^s y_{t+4}(1), \quad E_t^s \pi_t^*, \Big)$$

The measurement equation of the state space model is given by

$$\zeta_t = \boldsymbol{\gamma} + \mathbf{C}\xi_t + \mathbf{D}u_t \qquad \text{with} \quad u_t \sim \mathcal{N}(0, \mathbf{I}), \tag{A.5}$$

where

$$\mathbf{C} = \begin{pmatrix} 1 & \theta_s(1) & \theta_c(1) & 1 & 0 & 4 & 1 & & & & & & & \\ \vdots & \vdots & \vdots & \vdots & \vdots & \vdots & \vdots & & & & \mathbf{0_{K\times 7}} & & & \\ 1 & \theta_s(\tau_K) & \theta_c(\tau_K) & 1 & 0 & 4 & 1 & & & & & & & \\ 0 & 0 & 0 & 0 & 1 & 0 & 0 & 0 & 1 & 0 & 0 & 0 & 0 & 0 \\ 0 & 0 & 0 & 1 & 0 & 0 & 0 & 1 & 0 & 0 & 0 & 0 & 0 & 0 \\ & & & & & & \mathbf{C}_1\mathbf{F}^4 & & & & & & & \\ 0 & 0 & 0 & 1 & 0 & 0 & 0 & 0 & 0 & 0 & 0 & 0 & 0 & 0 \end{pmatrix} \tag{A.6}$$

$\mathbf{C}_1$ denotes the first row of $\mathbf{C}$. The matrix $\mathbf{D}$ is assumed to be diagonal with standard deviations of measurement innovations on their diagonal. Lastly, the column vector for the constants in the measurement equation $\boldsymbol{\gamma}$ is given by

$$\boldsymbol{\gamma} = \begin{pmatrix} \mathcal{A}(\tau_1) & \dots & \mathcal{A}(\tau_K) & 0 & 0 & \gamma^{shsr} & 0 \end{pmatrix}', \tag{A.7}$$

where $\gamma^{shsr} = \mathcal{A}(1) + \mathbf{C}_1(\mathbf{I} + \mathbf{F} + \mathbf{F}^2 + \mathbf{F}^3)\boldsymbol{\mu}$.

A.2 Estimated latent states

Figure A.1: Smoothed latent states

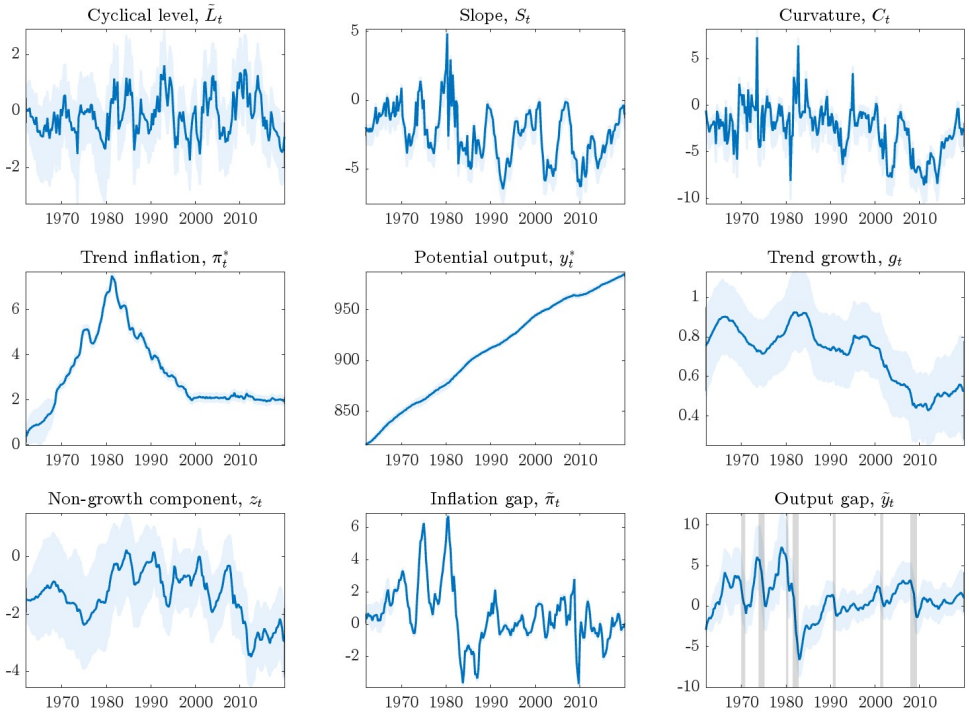

Note: The figure shows the posterior median of the latent states together with their 90% credible set.

A.3 Model-implied one-quarter ahead inflation expectations

Figure A.2 compares our posterior median model-implied one-quarter ahead inflation expectations, together with its 90% credible set, with the estimate from Holston et al. (2017) downloaded from the homepage of the New York Fed. Before comparing both series, note that our measure of short-term inflation expectations is based on the year-on-year growth in the consumer price index (variable `CPIAUCSL_PC1`, obtained from the Federal Reserve Bank of St. Louis's FRED database, or `CPALTT01USQ661S_PC1`, whereas Holston et al. (2017) base their estimate on the personal consumption expenditures index excluding food and energy (`DPCCRV1Q225SBEA`). The higher inflation expectations in the mid-1970s until early 1980s largely reflect differences in the year-on-year increases in CPI and core PCE. Similarly, in the last two decades of the sample (2000Q1-2019Q4), CPI inflation stood on average 0.44 percentage points above core PCE.

Figure A.2: Model-implied one-quarter ahead inflation expectations vs. HLW

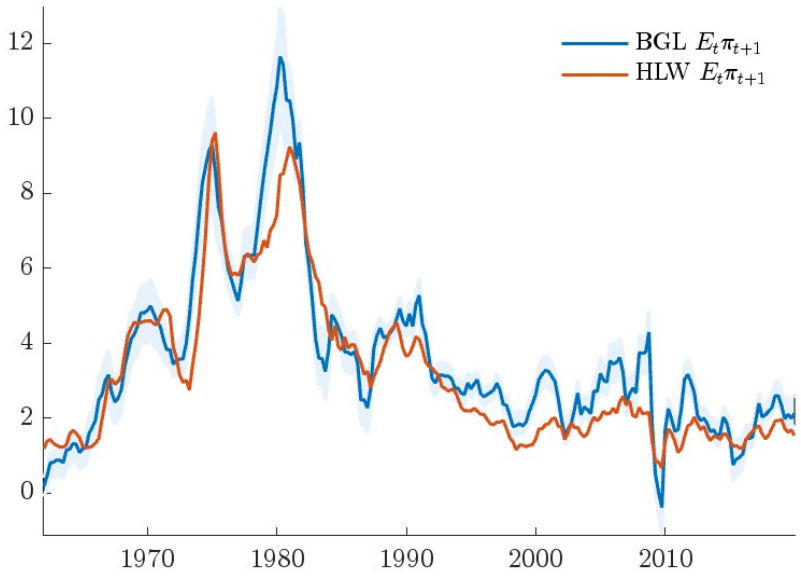

Note: The figure compares our posterior median one-quarter ahead inflation expectations together with its 90% credible set with the estimate from Holston et al. (2017) downloaded from the homepage of the New York Fed.

B Parameter restrictions to rule out arbitrage in the dynamic Nelson-Siegel model

In this section, we explain the derivation of the Nelson-Siegel yield equations from a no-arbitrage perspective, and in particular the adjustment term $\mathcal{A}(\tau)$ in the yield Equation (5). As shown by Christensen et al. (2011) and, in a discrete-time setting, Li et al. (2012), pricing bonds under a specific choice of risk-neutral factor dynamics renders the joint dynamics of bond yields arbitrage-free, gives rise to factor loadings having the Nelson-Siegel functional form, but implies an additional intercept term that is not present in the standard – statistically motivated – Nelson-Siegel formulation.

Starting from the definition of the state vector ξ_t as in Appendix A.1, we define a factor vector $F_t = [L_t, \bar{\xi}_t]$, where $\bar{\xi}_t$ equals our state vector ξ_t except that the first three elements are re-shuffled so that $\tilde{L}$ appears after the slope and curvature factor S and C. The so-constructed factor vector F_t has the three Nelson-Siegel factors L_t, S_t and C_t lining up upfront. Note further that L results as a linear combination of the states $\tilde{L}$, g, z and π^*.[28] We further group $F_t = [F_t^u F_t^m]$ with $F_t^u = [L_t, S_t, C_t]$ and F_t^m capturing the rest of the variables. Based on that partitioning of factors we represent the expression for the short-term interest rate, $i_t \equiv y_t(1)$, as

$$i_t = \delta_0 + \delta_u' F_t^u + \delta_m' F_t^m = \delta_0 + \delta' F_t \tag{B.8}$$

with obvious notation. Let $P_t(\tau)$ denote the time-t price of a zero-coupon bond with residual maturity τ. If there are risk-neutral factor dynamics (labeled by $\mathbb{Q}$)

$$F_t = c^{\mathbb{Q}} + \Phi^{\mathbb{Q}} F_{t-1} + v_t^{\mathbb{Q}}, \quad v_t^{\mathbb{Q}} \sim \mathcal{N}(0, \Omega) \tag{B.9}$$

so that bond prices satisfy

$$P_t(\tau) = e^{-i_t} E_t^{\mathbb{Q}} P_{t+1}(\tau - 1), \quad P_t(0) = 1,$$

then the joint evolution of bond prices is arbitrage-free. Moreover, the solution to the pricing

[28] Note: $L_t = \tilde{L}_t + i_t^* = \tilde{L}_t + 4g_t + z_t + \pi_t^*$.

equation is exponentially affine in factors

$$P_t(\tau) = \exp\left(a(\tau) + b(\tau)' F_t\right)$$

where coefficients $a(\tau)$ and $b(\tau)$ satisfy the well-known difference equations

$$a(\tau+1) = a(\tau) + b(\tau)' c^{\mathbb{Q}} + \frac{1}{2} b(\tau)' \Omega b(\tau) - \delta_0 \tag{B.10}$$

$$b(\tau+1)' = b(\tau)' \Phi^{\mathbb{Q}} - \delta', \tag{B.11}$$

with $a(1) = -\delta_0$ and $b(1) = -\delta$.

It is straightforward to see that if

$$\Phi^{\mathbb{Q}} = \begin{pmatrix} \Phi^{\mathbb{Q}}_{uu} & 0 \\ \Phi^{\mathbb{Q}}_{mu} & \Phi^{\mathbb{Q}}_{mm} \end{pmatrix}, \tag{B.12}$$

and $\delta' = [\delta'_u, 0, \ldots, 0]$, then $b(\tau) = [b_u(\tau)', 0, \ldots, 0]$, and the difference equations for the factor loadings reduce to the elements corresponding to the three factors,

$$a(\tau+1) = a(\tau) + b_u(\tau)' c^{\mathbb{Q}}_u + \frac{1}{2} b_u(\tau)' \Omega_{uu} b_u(\tau) - \delta_0 \tag{B.13}$$

$$b_u(\tau+1)' = b_u(\tau)' \Phi^{\mathbb{Q}}_{uu} - \delta'_u, \tag{B.14}$$

with $a(1) = -\delta_0$ and $b_u(1) = -\delta_u$.

Moreover, as shown by Li et al. (2012), if $\Phi^{\mathbb{Q}}_{uu}$ is of the form

$$\Phi^{\mathbb{Q}}_{uu} = \begin{pmatrix} 1 & 0 & 0 \\ 0 & e^{-\lambda} & \lambda e^{-\lambda} \\ 0 & 0 & e^{-\lambda} \end{pmatrix}, \tag{B.15}$$

and $\delta_u = [1, \frac{1-e^{-\lambda}}{\lambda}, -e^{-\lambda} + \frac{1-e^{-\lambda}}{\lambda}]'$ then $b(\tau)$ exhibits the specific Nelson-Siegel loadings (in price space) for the first three factors L, S and C (and zero on the other factors),

$$b(\tau) = \left[-\tau, -\frac{1-e^{-\lambda\tau}}{\lambda}, \tau e^{-\lambda\tau} - \frac{1-e^{-\lambda\tau}}{\lambda}, 0, \ldots, 0 \right]'. \tag{B.16}$$

Recalling that $F_t = [L_t, \bar{\xi}_t]$ is just an extension and permutation of our state vector ξ_t, the

transition equation for F_t is readily derived from that of ξ_t described in Section A.1 of the Appendix. It is affine, as the stipulated (unobserved) risk-neutral dynamics in (B.9) above, but depends on the physical (no $\mathbb{Q}$ label) parameters:

$$F_t = c + \Phi F_{t-1} + v_t, \quad v_t \sim \mathcal{N}(0, \Omega).$$

The variance-covariance matrix Ω of state innovations is the same under both the risk-neutral and the physical measure. For our factor vector $F_t = [L_t, \bar{\xi}_t]$ it follows from the dynamics of ξ_t and the link of L_t to $\tilde{L}$, z_t, g_t and π_t^* that Ω_{uu} in (B.13) is given by[29]

$$\Omega_{uu} = diag(\sigma_{\tilde{L}}^2 + \sigma_{\pi^*}^2 + 16\sigma_g^2 + \sigma_z^2, \sigma_s^2, \sigma_c^2),$$

where σ_i^2 denotes the variance of the innovation ε_t^i of variable i in our model. Parameters governing the risk-neutral and physical dynamics are linked as

$$c^{\mathbb{Q}} = c - \Omega^{\frac{1}{2}}\lambda_0, \quad \Phi^{\mathbb{Q}} = \Phi - \Omega^{\frac{1}{2}}\Lambda$$

where λ_0 and Λ ('market prices of risk') are a vector and a matrix, respectively, of appropriate dimension.

Mapping bond prices into yields using $y_t(\tau) = -\frac{1}{\tau}\ln P_t(\tau)$, we have

$$y_t(\tau) = \mathcal{A}(\tau) + \mathcal{B}(\tau)' F_t$$

where $\mathcal{A}(\tau) = -\frac{1}{\tau}a(\tau)$ and $\mathcal{B}(\tau) = -\frac{1}{\tau}b(\tau)$. That is, $\mathcal{B}(\tau)$ has now the Nelson-Siegel loadings as in equation (6) in the main text for bond yields as the first three entries, and $\mathcal{A}(\tau)$ is the intercept appearing in (5).

The risk-neutral dynamics and cross-sectional pricing equations are parsimoniously parameterized. The relevant variance-covariance matrix Ω_{uu} is implied by the time series estimates under the physical measure as explained above. As we are working with latent factors, the parameter δ_0 in the short-rate equation is not identified and can be arbitrarily calibrated. While it is common to set it to zero, we choose to set $\delta_0 = -\theta_s(1)\bar{S} - \theta_c(1)\bar{C}$ so that (as $a(1) = -\delta_0$) $\mathcal{A}(1) = -a(1) = -\theta_s(1)\bar{S} - \theta_c(1)\bar{C}$ as specified in the main text. Finally, we set the risk-neutral

[29] For instance, the first term follows from collecting the innovation terms for $L_t = \tilde{L}_t + i_t^* = \tilde{L}_t + 4g_t + z_t + \pi_t^*$.

VAR intercept $c^{\mathbb{Q}}$ equal to zero. This is a somewhat ad-hoc choice to prevent additional parameters to enter our setup and is tantamount to imposing a restriction on the market price of risk vector λ_0, given the estimates of c and Ω of the physical dynamics. While under that specific choice of $c^{\mathbb{Q}}$ model-implied bond yield dynamics are arbitrage-free, it is eventually an empirical question, whether $c^{\mathbb{Q}} = 0$ is an overly restrictive assumption. Via its impact on $\mathcal{A}(\tau)$, the choice of $c^{\mathbb{Q}}$ affects the (average) slope of the yield curve as argued in the main text. It turns out empirically that the model fits the average slope in the data fairly well so that the parameter restriction appears non-problematic from this perspective.

C Unit root tests of DNS factors

Table C.1 presents the results of augmented Dickey Fuller tests for empirical measures of level, slope and curvature as well as factors calculated based on a DNS model with $\lambda = 3 \times 0.0607$, both as suggested in Diebold and Li (2006). As evident from the table, unit root tests clearly reject the null hypothesis of a unit root in slope and curvature for the US.

Table C.1: Unit root tests for the yield curve factors

Measure	Reject	*p*-value	Test Statistic	Lags
Emp. level	0	0.6134	-1.312	0
	0	0.6273	-1.191	1
	0	0.6686	-1.147	2
	0	0.5771	-1.255	3
	0	0.6487	-1.298	4
Emp. slope	1	0.0082	-3.539	0
	1	0.0359	-3.006	1
	1	0.0292	-3.086	2
	1	0.0075	-3.569	3
	1	0.007	-3.594	4
Emp. curvature	1	0.001	-6.004	0
	1	0.001	-4.44	1
	1	0.0032	-3.89	2
	1	0.0154	-3.315	3
	1	0.0163	-3.298	4
DNS level	0	0.6134	-1.281	0
	0	0.6273	-1.249	1
	0	0.6686	-1.156	2
	0	0.5771	-1.363	3
	0	0.6487	-1.201	4
DNS slope	1	0.001	-4.3	0
	1	0.0062	-3.629	1
	1	0.0164	-3.296	2
	1	0.0014	-4.103	3
	1	0.0026	-3.961	4
DNS curvature	1	0.001	-5.307	0
	1	0.0022	-4.012	1
	1	0.0074	-3.573	2
	1	0.0266	-3.12	3
	1	0.0243	-3.153	4

Note: As suggested by Diebold and Li (2006), empirical measures for the level, (negative) slope and curvature are the 10-year bond yield, the 2-year yield minus the 10-year yield and two times the 2-year yield less the 3-months rate and the 10-year yield. A value of 1 (0) in the column "Reject" means that the null hypothesis of a unit root is rejected (not rejected) at the 5% significance level. Lags specifies the number of lagged difference terms in the alternative model.

D MCMC algorithm

Let Θ denote the vector of all model parameters (except the DNS parameter λ):

$$\Theta = \begin{pmatrix} a_1 & a_2 & a_3 & b_1 & b_2 & a_L & a_{10} & a_{11} & a_{12} & a_{13} & a_{14} & a_{20} & a_{21} & a_{22} & a_{23} & a_{24} & \dots \\ & & & & \dots & \sigma^2_{lc} & \sigma^2_{s} & \sigma^2_{c} & \sigma^2_{\pi^*} & \sigma^2_{x^*} & \sigma^2_{\bar{\pi}} & \sigma^2_{\bar{x}} & \sigma^2_{\tau_2} & \dots & \sigma^2_{\tau_{13}} & \sigma^2_{s,\pi} & \sigma^2_{s,shsr} \end{pmatrix}.$$

MCMC estimates of the model are obtained from a Gibbs sampler. The Gibbs sampler generates draws from the joint posterior distribution of states ξ_t and parameters Θ and λ given the observables ζ, denoted $p(\xi, \Theta, \lambda|\zeta)$. The sampler is initialized with parameter values drawn from their respective priors. Initial states, ξ_0, for the simulation smoother are based on estimates

from a two-sided HP-filter with a standard deviation of 0.25. It then loops over the following steps:

1. Draw $\xi = \{\xi_1, \ldots, \xi_T\}$ from $p(\xi|\Theta, \lambda, \zeta)$: Conditional on the parameters Θ and λ, construct matrices $\mathbf{C}, \mathbf{D}, \mathbf{F}$ and $\mathbf{G}$ to obtain a linear Gaussian state space model. Conditional on the observables $\zeta = \{\zeta_1, \ldots, \zeta_T\}$, draw the states ξ using the Durbin Koopmans simulations smoother.

2. Draw Θ from $p(\Theta|\lambda, \xi, \zeta)$: Using Bayesian recursive regressions, draw parameters Θ from their Normal Inverse Gamma or Normal Inverse Wishart distributions, respectively, rejecting parameter draws that would render the dynamics of cyclical states non-stationary. This amounts to a set of 11 regressions, which can be sampled independently since the errors are assumed to be mutually orthogonal.

3. Draw λ from $p(\lambda|\Theta, \xi, \zeta)$: The measurement equations for all yields depend on λ in a nonlinear fashion. As a consequence, the distribution of λ is non-standard and cannot be sampled from directly. To draw a new λ, we use the following random walk Metropolis Hastings step:

$$\lambda^* = \lambda^{(i-1)} + Z\sqrt{\Sigma_\lambda},$$

where λ^* denotes the proposal, and $\lambda^{(i-1)}$ denotes the last accepted draw of λ and $Z \sim \mathcal{N}(0, 1)$. Next, compute the acceptance probability as

$$\alpha = \min\left(\frac{p(\zeta|\Theta, \lambda^*, \xi)}{p(\zeta|\Theta, \lambda^{(i-1)}, \xi)}, 1\right),$$

with

$$p(\zeta|\Theta, \lambda, \xi) \propto \exp\left(\sum_{t=1}^{T}\left[\zeta_t - \boldsymbol{\gamma}(\lambda) - \mathbf{C}(\lambda)\xi_t\right]\right).$$

With probability α, we accept the new threshold value and set $\lambda^{(i)} = \lambda^*$. Otherwise, we set $\lambda^{(i)} = \lambda^{(i-1)}$. The variable Σ_λ is the scale of the Metropolis Hastings step, and is tuned to ensure an acceptance rate between 20 - 40 percent.

4. Repeat steps 1-3 until convergence.

The results presented are based on one single chaien with a total of 100,000 draws of which we use the first 90,000 as burn-in and subsequently retain every tenth draw of the remaining

10,000. The thinning of the posterior sample eliminates any residual sample autocorrelation in the Gibbs sampler. Convergence is checked on the basis of recursive means as proposed by Geweke (1991). We also confirmed convergence by having multiple chains starting from different initial values and merging the resulting post-burn-in draws. In the Appendix E below, we show that the posterior distributions resulting from a single or multiple chains are virtually equivalent.

E Posterior plots

Figure E.1: Prior and posterior distributions of model coefficients

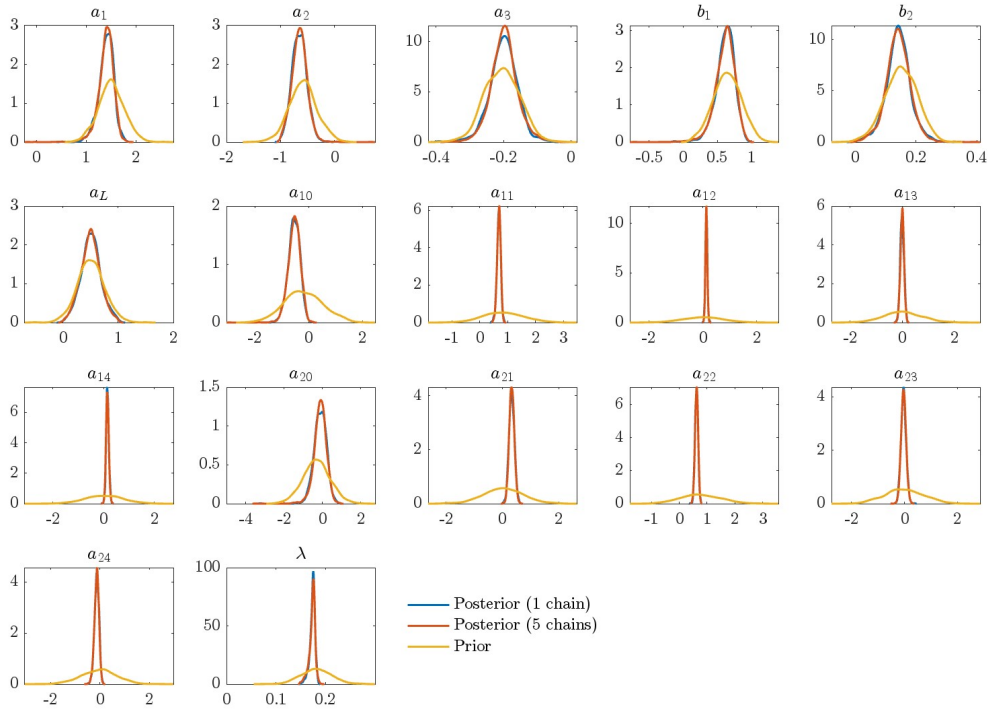

Note: The figure shows the prior distributions of the model parameters in yellow, together with the posterior distributions based on a single chain in blue, or based on five chains in red. Each chain comprises 100,000 iterations of which the first 90,000 were burn-in and of the remaining 10,000 every 10th draw was retained. For multiple chains, the posterior pools all retained draws.

Figure E.2: Prior and posterior distributions of standard deviations

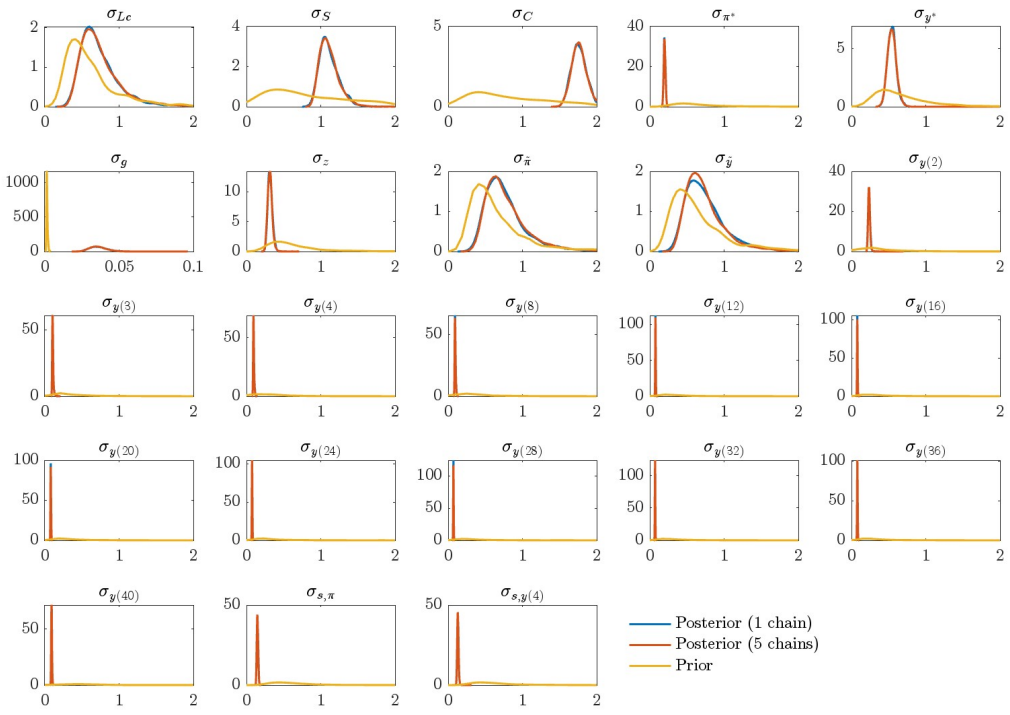

Note: The figure shows the prior distributions of the model standard deviations in yellow, together with the posterior distributions based on a single chain in blue, or based on five chains in red. Each chain comprises 100,000 iterations of which the first 90,000 were burn-in and of the remaining 10,000 every 10th draw was retained. For multiple chains, the posterior pools all retained draws.

F Inference using partial data

The main text discusses three ways to assess the relevance of the different measurement data for the estimation of r_t^*. The first applies the historical data decomposition of Koopman and Harvey (2003) which expresses the estimated latent states in terms of contributions from observed variables. The second is a filtering (and smoothing) exercise using only a subset of the data and taking the posterior median coefficient estimates as given. The third (see Section 5.3 in the main text or J.2 below) re-estimates the full model with only short-rate (as opposed to full yield curve) information closing the model.

This section provides additional figures on the inference of r_t^* for the second exercise. Specifically, in the first column, Figure F.1 shows the posterior median estimate of r_t^* if we *exclude* macro data (top), financial data (middle), or survey data (bottom) and compares it to the "full information" baseline. As is evident from the figures, all three data sources are used to determine

the level of the natural rate. Two specific observations stand out: First, the version without financial data, gives rise to mostly higher and significantly smoother r^* estimates throughout the first three decades of the sample, confirming our conjecture that closing the model with an endogenous interest rate equation generates more cyclical r^* estimates and thereby less persistent real rate gap measures, especially in this part of the sample. Second, we observe that including survey information gives rise to significantly higher r^* estimates during the Great Inflation period of the 1970s, and significantly lower estimates during the ZLB episode. This is because, in the 1970s, surveys measures for long-run inflation expectations help to anchor trend inflation, whereas survey-based short-term interest expectations anchor model-implied short-rate expectations closer to the ELB akin to Geiger and Schupp (2018).

Looking at the effect on estimation uncertainty, as proxied by the 95th-5th interpercentile range, we can observe that macro economic data is particularly useful following the Great Moderation, while financial data helps to reduce estimation uncertainty during the 1970s and 80s. Surveys, in turn, are generally important to inform latent states, with their increasing effect on the precision reflecting the fact that interest rate surveys only become available as of 1990Q1.

Figure F.1: Smoothed estimates of r_t^* using partial data

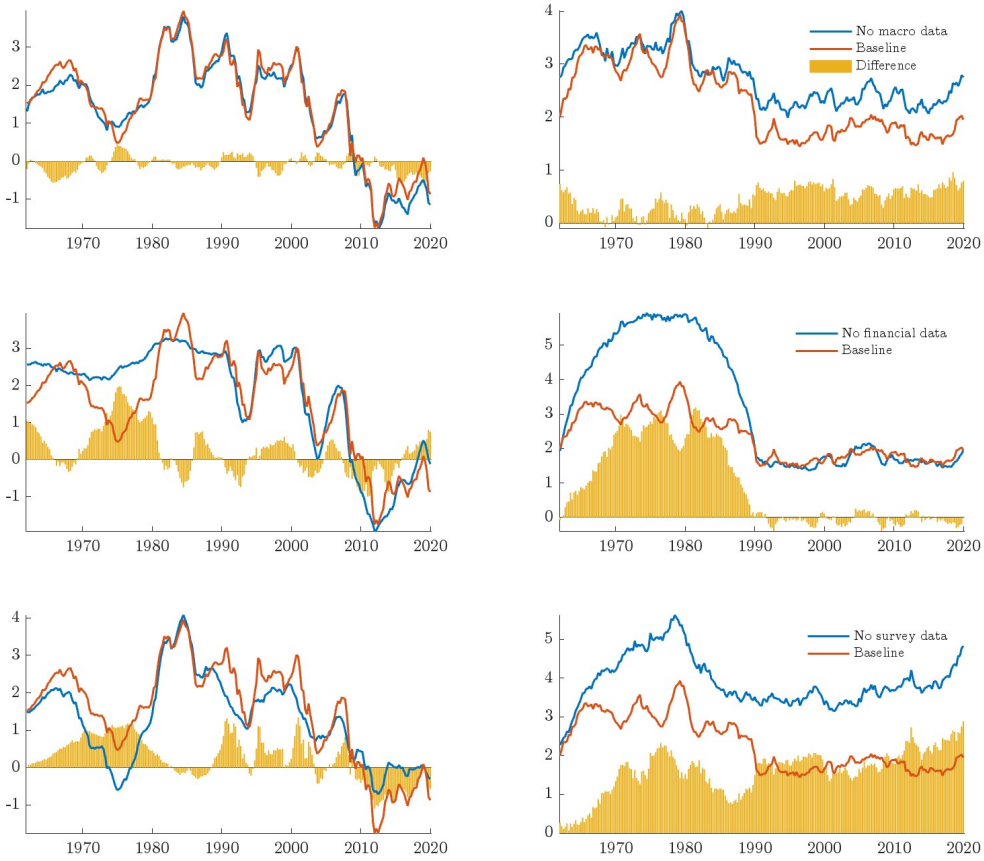

Note: The figure shows the posterior median r_t^* estimate (left column) together with the width of the 95th-5th interpercentile range (right column) if we (i) drop macro data (upper panels), (ii) drop financial data (middle panels), (iii) drop survey data (bottom panels), and compares it to the full information baseline. Posterior parameter estimates are taken as given.

G The natural yield curve as benchmark for the actual yield curve

As touched upon in Section 2.2 of the main text, our model implies a natural yield curve, i.e. a long-run attractor for yields of all maturities, whose location varies over time with the stochastic drift in the level factor. This section gives an idea of how the natural yield curve can be used as a benchmark for the actual yield curve.

Figure G.1 shows the natural yield curve at three points in time and compares it with the respective observed yield curve. Note that both the actual and natural curve are expressed in

terms of nominal interest rates. We can thus interpret the natural curve as a "benchmark" for the actual curve, in the sense that the latter is expected to converge to the former in the absence of further shocks. However, we cannot use the difference between the two as a measure of monetary policy stance *stricto sensu*, which would require using the term structure of *real* interest rates.[30]

The left panel of Figure G.1 depicts the yield curve (red) in June 2006, i.e. near the end of a Fed tightening cycle that had started in July 2004 from a level of the federal funds rate around one percent. The three-month rate in June 2006 was around 5.2%, and thereby around 4 percentage points higher than two years earlier and, according to our estimates, clearly above the natural nominal interest rate. At the same time, the relatively flat and slightly inverted yield curve implied that the long-term rate at that time would be close to its neutral level (red curve for longer maturities within the blue credibility range for the natural yield curve).

Three and a half years later (end-December 2009, middle panel of Figure G.1), the Federal Reserve had reacted with a sequence of rate cuts to address the economic fallout of the GFC: the nominal short-term rate was near zero, while the yield curve was steep with ten-year rates standing at above 4%. Comparing again to the estimated natural yield curve, the policy rate cuts had brought the actual short-term rate clearly below its natural counterpart, in line with the intended loose monetary policy stance. The long-term rate would have also been on the loose side when being compared to our initial natural yield curve of mid-2006 (left panel). However, over time, the nominal natural curve is estimated to have also shifted down (in line with the natural short-term real rate decline after the GFC, as discussed above) so that an actual ten-year rate level of 4% stood above its neutral level in December 2009.

Another three years later in December 2012 the short-term nominal interest rate was still near its zero lower bound (and it would turn out to stay there for another three years), see right panel of Figure G.1. At the same time, the estimated natural curve has declined further, but the short rate remained in "loose" territory as it ranged below the point estimate of the natural nominal rate of around 0.6% at that time. The overall yield curve was flatter in December 2012 compared to three years earlier, reflecting *inter alia* expectations by market participants that policy rates would stay low for an extended period of time and the Fed's quantitative easing.[31]

[30] In Section 5.1 we show that it is intricate to compute model-consistent long-term real rates. First, computing the term structure of inflation expectations requires solving a fixed-point problem with some small modifications to the model. Second, deflating nominal yields with thus-computed inflation expectations still ignores inflation risk premia which should enter a proper computation of real rates when starting from nominal rates.

[31] Incorporating QE explicitly into our framework would require significant changes to our model and its es-

Relative to our point estimate of the natural curve, the whole term structure of actual nominal rates was ranging below its natural counterpart, falling even below its 90% credible set for intermediate maturities.

Overall, this exercise highlights the importance of taking into account time variation in low-frequency trends when assessing the level of the yield curve. The same level of the curve may be deemed "high" when occurring in an environment of a low natural curve, but it would rather reflect an environment of overall favorable nominal financing conditions at a time when the natural curve is higher.

Figure G.1: Observed and natural yield curve at different points in time

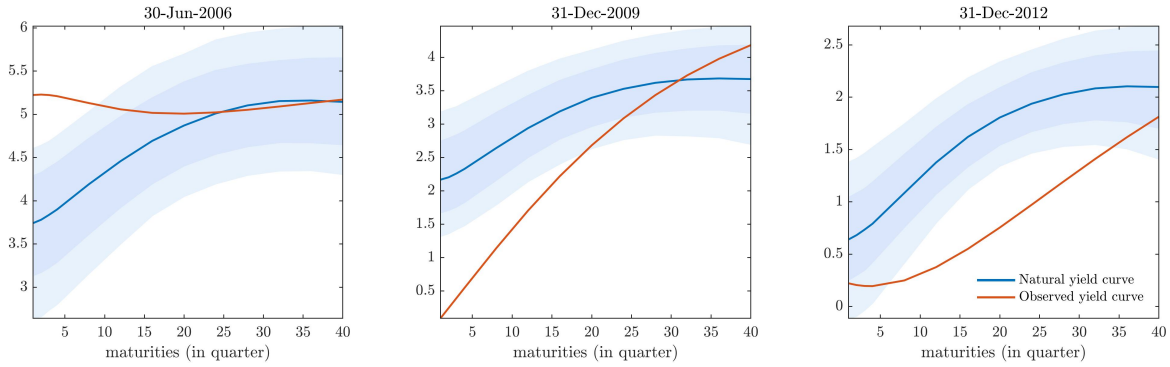

Note: The figure shows the natural yield curve, together with its 68% and 90% credible set, and compares it to the observed yield curve.

H Model version with long-term rates entering the IS curve

This section presents the state space representation of the model version in which a long-term (as opposed to a one-period) real-rate gap enters the IS curve. After the model derivations we also show that our model-implied measure of real rates align fairly well with real rates of inflation-linked bonds ("TIPS rates").

As introduced in the main text, for any maturity τ, we assume the IS curve (1) of the baseline

timation. See, e.g., Li and Wei (2013) on how to modify a standard yield curve model in order to incorporate forward-looking bond supply shocks. We leave such an extension to future research.

model is replaced by[32]

$$\tilde{x}_t = a_1\tilde{x}_{t-1} + a_2\tilde{x}_{t-2} + a_3 E_{t-1}\sum_{l=1}^{2}\left[y_{t-l}(\tau) - \frac{1}{\tau}\sum_{j=1}^{\tau}\pi_{t-l+j} - \left(y^*_{t-l}(\tau) - \frac{1}{\tau}\sum_{j=1}^{\tau}\pi^*_{t-l+j}\right)\right] + \varepsilon^{\tilde{x}}_t. \tag{H.17}$$

All other equations remain unchanged. To derive the state space representation, substitute (5) and (14) into (H.17) to find

$$\begin{aligned}
\tilde{x}_t \;=\;& a_3\tilde{L}_{t-1} + a_3\theta_s(\tau)S_{t-1} + a_3\theta_c(\tau)C_{t-1} \\
& -\frac{a_3}{2\tau}\tilde{\pi}_{t-1} + a_1\tilde{x}_{t-1} \\
& +a_3\tilde{L}_{t-2} + a_3\theta_s(\tau)S_{t-2} + a_3\theta_c(\tau)C_{t-2} \\
& +a_2\tilde{x}_{t-2} \\
& -\frac{a_3}{\tau}\left(\sum_{j=1}^{\tau-1}E_{t-1}\tilde{\pi}_{t+j-1} + \frac{1}{2}E_{t-1}\tilde{\pi}_{t+\tau-1}\right) \\
& -a_3\left(\theta_s(\tau)\bar{S} + \theta_c(\tau)\bar{C}\right).
\end{aligned}$$

The state transition equation will therefore be of the following form

$$\xi_t = \boldsymbol{a} + \boldsymbol{A}_0\xi_{t-1} + \boldsymbol{A}_1 E_{t-1}\xi_t + ... + \boldsymbol{A}_\tau E_{t-1}\xi_{t+\tau-1} + \mathbf{G}e_t, \tag{H.18}$$

where $\mathbf{G}e_t$ is the same as in the state space representation of the baseline model, see Annex section A.1. The state vector ξ_t (repeated here for convenience) remains

$$\xi_t = \begin{pmatrix}\tilde{L}_t & S_t & C_t & \pi^*_t & x^*_t & g_t & z_t & \tilde{\pi}_t & \tilde{x}_t & \tilde{L}_{t-1} & S_{t-1} & C_{t-1} & \tilde{\pi}_{t-1} & \tilde{x}_{t-1}\end{pmatrix}'.$$

The vector of constant terms is given by

$$\boldsymbol{a} = \begin{pmatrix}0 & a_{10} & a_{20} & 0 & 0 & 0 & 0 & 0 & -a_3[\theta_s(\tau)\bar{S} + \theta_c(\tau)\bar{C}] & 0 & 0 & 0 & 0 & 0\end{pmatrix}',$$

[32] To avoid keeping track of past inflation expectations as extra state variables we assume that both real rate gaps are conditional on the $t-1$ information set, which eases the calculation substantially.

and the respective matrices for lagged and expected states are given by

$$\boldsymbol{A}_0 = \begin{pmatrix}
a_L & 0 & 0 & 0 & 0 & 0 & 0 & 0 & 0 & & & & & \\
0 & a_{11} & a_{12} & 0 & 0 & 0 & 0 & a_{13} & a_{14} & & \mathbf{0_{3\times 5}} & & & \\
0 & a_{21} & a_{22} & 0 & 0 & 0 & 0 & a_{23} & a_{24} & & & & & \\
 & & & 1 & 0 & 0 & 0 & & & & & & & \\
 & \mathbf{0_{4\times 3}} & & 0 & 1 & 1 & 0 & & & & & \mathbf{0_{4\times 7}} & & \\
 & & & 0 & 0 & 1 & 0 & & & & & & & \\
 & & & 0 & 0 & 0 & 1 & & & & & & & \\
0 & 0 & 0 & 0 & 0 & 0 & 0 & b_1 & b_2 & 0 & 0 & 0 & 0 & 0 \\
a_3 & a_3\theta_s(\tau) & a_3\theta_c(\tau) & 0 & 0 & 0 & 0 & -\frac{a_3}{2\tau} & a_1 & a_3 & a_3\theta_s(\tau) & a_3\theta_c(\tau) & 0 & a_2 \\
 & \mathbf{I_{3\times 3}} & & & & & & & & & \mathbf{0_{3\times 11}} & & & \\
 & & & \mathbf{0_{2\times 7}} & & & & \mathbf{I_{2\times 2}} & & & & & \mathbf{0_{2\times 5}} &
\end{pmatrix},$$

$$\boldsymbol{A}_i = \begin{pmatrix} & & & & & & & & \mathbf{0_{8\times 14}} & & & & & & & \\ 0 & 0 & 0 & 0 & 0 & 0 & 0 & -\frac{a_3}{\tau} & 0 & 0 & 0 & 0 & 0 & 0 & 0 & 0 \\ & & & & & & & & \mathbf{0_{5\times 14}} & & & & & & & \end{pmatrix}, \qquad \forall i = 1, ..., \tau - 1,$$

$$\boldsymbol{A}_\tau = \begin{pmatrix} & & & & & & & & \mathbf{0_{8\times 14}} & & & & & & & \\ 0 & 0 & 0 & 0 & 0 & 0 & 0 & -\frac{a_3}{2\tau} & 0 & 0 & 0 & 0 & 0 & 0 & 0 & 0 \\ & & & & & & & & \mathbf{0_{5\times 14}} & & & & & & & \end{pmatrix}.$$

To solve the model, we guess that the non-stochastic part of the solution is linear in states

$$\xi_t = \boldsymbol{\mu} + \mathbf{F}\xi_{t-1}.$$

Then, the $k+1$-period forecast is given by

$$E_{t-1}\xi_{t+k} = (\boldsymbol{\mu} + \mathbf{F}\boldsymbol{\mu} + ... + \mathbf{F}^k\boldsymbol{\mu}) + \mathbf{F}^{k+1}\xi_{t-1}.$$

Substitution yields

$$\begin{aligned}\xi_t =& \boldsymbol{a} + A_0\xi_{t-1} + A_1\big(\boldsymbol{\mu} + \mathbf{F}\xi_{t-1}\big) + A_2\big(\boldsymbol{\mu} + \mathbf{F}\boldsymbol{\mu} + \mathbf{F}^2\xi_{t-1}\big) + ... + A_\tau[(\boldsymbol{\mu} + \mathbf{F}\boldsymbol{\mu} + ... + \mathbf{F}^{\tau-1}\boldsymbol{\mu}) + \mathbf{F}^\tau\xi_{t-1}] \\ =& \boldsymbol{a} + \sum_{i=1}^{\tau} A_i\left(\sum_{j=1}^{i}\mathbf{F}^{j-1}\boldsymbol{\mu}\right) + \left(A_0 + \sum_{i=1}^{\tau}A_i\mathbf{F}^i\right)\xi_{t-1} + \mathbf{G}e_t,\end{aligned}$$

which confirms our initial guess and yields a set of implicit and nonlinear mappings for parameter

vectors and matrices $\boldsymbol{\mu}$ and $\mathbf{F}$:

$$\mathbf{F} = A_0 + \sum_{i=1}^{\tau} A_i \mathbf{F}^i, \tag{H.19}$$

$$\boldsymbol{\mu} = \boldsymbol{a} + \sum_{i=1}^{\tau} A_i \left(\sum_{j=1}^{i} \mathbf{F}^{j-1} \boldsymbol{\mu} \right). \tag{H.20}$$

Vectorizing (H.19) yields

$$vec(\mathbf{F}) = vec(\mathbf{A}_0) + \sum_{i=1}^{\tau} \left(\mathbf{I}_n \otimes \mathbf{A}_i \mathbf{F}^{i-1} \right) vec(\mathbf{F}).$$

Because (H.19) is an exponential matrix equation, multiple solutions may exist. We restrict ourselves to solutions with the maximum eigenvalue equal to exactly unity for the random walk processes. In contrast, $\boldsymbol{\mu}$ is uniquely pinned down by (H.20) for any given $\mathbf{F}$. Solving (H.20) for $\boldsymbol{\mu}$ yields

$$\boldsymbol{\mu} = \left(\mathbf{I} - \sum_{i=1}^{\tau} A_i \left[\sum_{j=1}^{i} \mathbf{F}^{j-1} \right] \right)^{-1} \boldsymbol{a}.$$

Finally, also the state-space representation of the model with long-term rates in the IS curve can be written in the form

$$\begin{aligned} \zeta_t &= \gamma + \mathbf{C}\xi_t + \mathbf{D}u_t \qquad \text{with} \quad u_t \sim \mathcal{N}(0, \mathbf{I}) \\ \xi_t &= \boldsymbol{\mu} + \mathbf{F}\xi_{t-1} + \mathbf{G}e_t \qquad \text{with} \quad e_t \sim \mathcal{N}(0, \mathbf{I}), \end{aligned}$$

with the new matrix $\mathbf{F}$ and intercept $\boldsymbol{\mu}$ as introduced in this sub-section, and with the remaining objects being unchanged compared to the baseline case.

Finally, as discussed in the main text, the real rate concept used in the gap measure is somewhat different from a long-term real rate as implied by inflation-linked bonds: conceptually, the measure used here is the long-term nominal rate minus average inflation expectations, while an inflation-linked bond rate would additionally subtract the corresponding inflation risk premium.

Accordingly, we cross-check by how much our model-based real rates differ empirically from readings of real rates of Treasury Inflation-Protected Securities (TIPS) as obtained from Gürkaynak et al. (2010). Figure H.1 suggests that our real rates align pretty well with TIPS rates, and surprisingly do so increasingly well for higher maturities. Table H.1 further confirms

this conclusions: except some level differences at shorter maturities, our real rates and TIPS align closely in both levels and variation as also underlined by high correlations.

Figure H.1: Model-implied real rates vs. TIPS

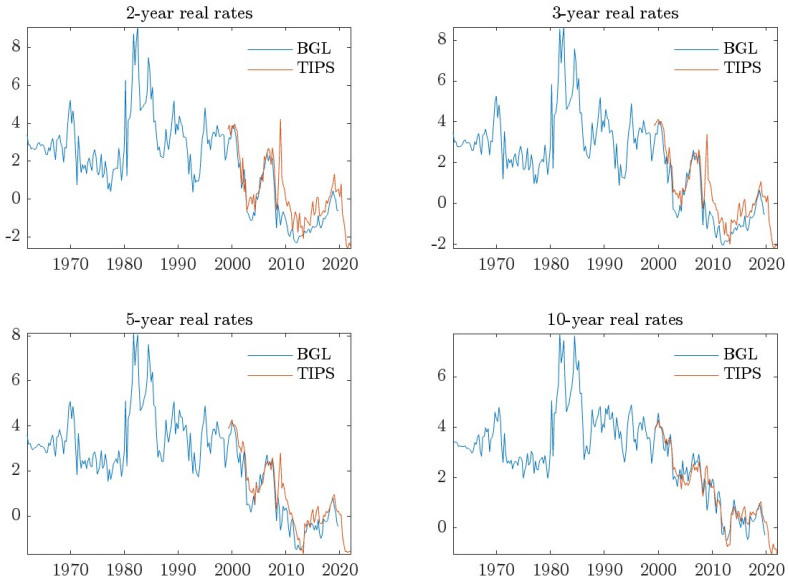

Note: Model-implied real rates are calculated as (fitted) nominal yield minus model-implied average inflation expectations. TIPS are based on Gürkaynak et al. (2010) and downloaded from the homepage of the Federal Reserve Board.

Table H.1: Comparative statistics: Model-implied real rates vs. TIPS

maturity (in years)	2	3	5	10
mean(BGL)	-0.14	0.16	0.68	1.54
mean(TIPS)	0.56	0.78	1.1	1.59
std(BGL)	1.69	1.65	1.5	1.33
std(TIPS)	1.59	1.55	1.48	1.27
std(Δ BGL)	0.5	0.52	0.51	0.45
std(ΔTIPS)	0.81	0.59	0.46	0.33
corr(BGL,TIPS)	0.88	0.91	0.93	0.96

I ELB extension

This section provides additional information about the extension of the baseline model to allow for the effective lower bound (ELB). As described in the main text, we follow Feunou et al. (2022). The shadow rate s_t is an affine function of the state vector, $s_t = \delta_1' \xi_t$, with δ_1 – in our

Figure I.1: Mapping between shadow rate and short-term rate for different values of shape parameter θ

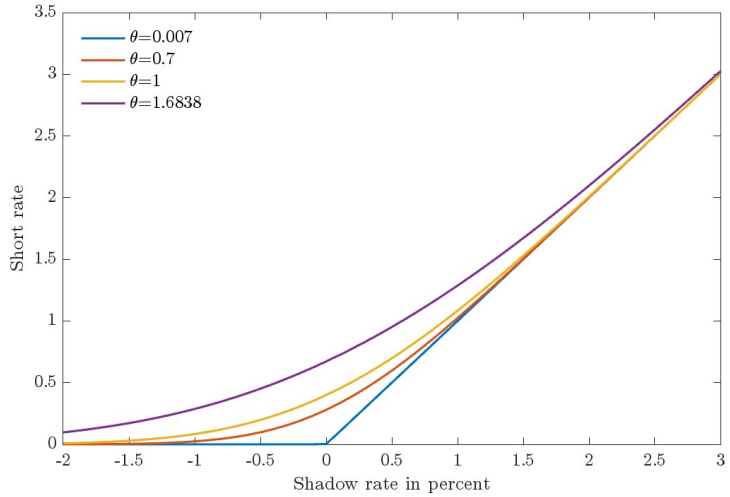

Note: Illustration of the mapping between the shadow rate and the short-term rate in Equation (20) for different values of θ.

case – being given by

$$\delta_1 = \begin{pmatrix} 1 & \frac{1-\exp(-\lambda)}{\lambda} & \frac{1-\exp(-\lambda)}{\lambda} - \exp(-\lambda) & 1 & 0 & 4 & 1 & 0 & 0 & 0 & 0 & 0 & 0 & 0 \end{pmatrix}.$$

The ELB constraint is approximated using a smooth nonlinear function $\omega(x)$ which maps the shadow rate s_t into the observed short-term rate $i_t \equiv y_t(1)$. This non-linear mapping shown in equation (20) in the main text is repeated here for convenience:

$$i_t = \theta\omega\left(\frac{s_t}{\theta}\right), \tag{I.21}$$

where $\theta > 0$ is a scalar, the function $\omega(\cdot)$ is defined as $\omega(x) = x\Phi(x) + \phi(x)$, and where Φ and ϕ are the cumulative distribution function and the probability density function of a standard normal distribution, respectively. Figure I.1 provides an illustration of the mapping between the shadow rate and the short-term rate for different values of θ. Independent of the specific shape of the function, governed by θ, the short-rate converges to the ELB for sufficiently negative levels of the shadow rate, while $s_t \approx i_t$ when s_t is distinctly above the ELB. Incorporating this ELB-preserving specification of the short rate, Feunou et al. (2022) derive a term structure of "close to arbitrage-free" bond prices and yields that is analytically tractable and can be parameterised to

be close to our no-arbitrage Nelson-Siegel specification for the linear (ignoring the ELB) baseline model. Specifically, they assume[33] that zero-coupon bond prices of maturity τ as a function of the state ξ_t are given by

$$P_t^\tau(\xi_t) = P_t^{\tau-1}(K\xi_t) \cdot e^{-m(\xi_t)}, \quad P_t^0 = 1, \quad \tau = 1, 2, \ldots \tag{I.22}$$

and show that this structure renders the family of bond prices almost arbitrage-free. In our application $m(\xi)$ is the mapping from the state to the short-term rate implied by (I.21), and K is chosen as the $N \times N$ matrix

$$K = \begin{pmatrix} 1 & 0 & 0 & 0 & 0 & 0 & 0 & \\ 0 & \exp(-\lambda) & \lambda\exp(-\lambda) & 0 & 0 & 0 & 0 & \\ 0 & 0 & \exp(-\lambda) & 0 & 0 & 0 & 0 & \\ 0 & 0 & 0 & 1 & 0 & 0 & 0 & \\ 0 & 0 & 0 & 0 & 0 & 0 & 0 & \\ 0 & 0 & 0 & 0 & 0 & 1 & 0 & \mathbf{0_{7\times 7}} \\ 0 & 0 & 0 & 0 & 0 & 0 & 1 & \\ & & & & \mathbf{0_{7\times 14}} & & & \end{pmatrix}.$$

Feunou et al. (2022) further show that under assumption (I.22), the one-quarter forward rate τ periods ahead is given by

$$f_t(\tau) = \theta\omega\left(\frac{\delta_1' K^\tau \xi_t}{\theta}\right). \tag{I.23}$$

where the expression in the enumerator can be interpreted as a shadow forward rate $s_t(\tau) = \delta_1' K^\tau \xi_t$. Using the forward rates, spot rates follow as

$$y_t(\tau) = \frac{1}{\tau}\sum_{i=0}^{\tau-1} f_t(i) = \frac{1}{\tau}\sum_{i=0}^{\tau-1} \theta\omega\left(\frac{\delta_1' K^i \xi_t}{\theta}\right) \equiv Z(\tau, \xi_t).$$

Our specific choice of K ensures that bond yields behave very similarly to those in our linear baseline model when the short rate is sufficiently positive.

Adding a measurement error,

$$y_t(\tau) = Z(\tau, \xi_t) + \varepsilon_t^\tau \tag{I.24}$$

[33] We adapt our notation, writing P_t^τ instead of $P_t(\tau)$ to make room for the state argument.

constitutes the nonlinear measurement equation pertaining to yields.

Estimation is done using the extended Kalman filter (EKF) with a simulation step in the spirit of Carter and Kohn (1994) to carry out Bayesian inference. For the updating step of the EKF, we need the Jacobian of Z with respect to the state vector ξ_t:

$$\frac{dZ(\tau,\xi)}{d\xi} = \frac{1}{\tau}\sum_{i=0}^{\tau-1}\theta\frac{d}{d\xi}\omega\left(\frac{\delta_1' K^i \xi_t}{\theta}\right) = \frac{1}{\tau}\sum_{i=0}^{\tau-1}\delta_1' K^i \Phi\left(\frac{\delta_1' K^i \xi_t}{\theta}\right),$$

where the last equality follows from the convenient result that

$$\omega'(x) = x\Phi'(x) + \Phi(x) - x\phi(x) = \Phi(x), \tag{I.25}$$

which applies the product rule for derivatives and uses an established results for the derivatives of normal probability density function and cumulative density function.

Lastly, the inclusion of the survey forecasts of the short-term rate four quarters ahead implies a measurement equation of the following type

$$E_t^s y_{t+4}(1) = E_t y_{t+4}(1) + u_t^{s,sr} = \theta E_t\left[\omega\left(\frac{s_{t+4}}{\theta}\right)\right] + u_t^{s,sr}.$$

Yet this expression involves the conditional expectation of a nonlinear function of a (conditionally normally distributed) random variable. Since there is no closed-form solution for it, we take a second-order approximation of that term to get an approximate measurement equation of which in turn can take the Jacobian required in the filtering step of the EKF.[34]

Specifically, for any nonlinear function $g(x)$ the second order Taylor approximation around a point $x = a$ is

$$g(x) \approx g(a) + g'(a)(x-a) + \frac{1}{2}g''(a)(x-a)^2.$$

If x is a random variable and we linearize around the expectation $a = E(x)$ (in our specific case, this will be the conditional expectation E_t), then, when taking expectations, $E[g(x)]$, the linear term disappears (as $E(x-a) = 0$), leaving us with the approximation for the expectation

$$E[g(x)] \approx g(a) + \frac{1}{2}g''(a)E[(x-a)^2] = g(a) + \frac{1}{2}g''(a)Var(x).$$

[34] An illustration that the approximation works well can be provided upon request.

To make this operationalizable, we need the second derivative of $\omega(x)$, which follows from (I.25) and is simply $\omega''(x) = \phi(x)$. Thus, we have

$$E_t\left[\omega\left(\frac{s_{t+4}}{\theta}\right)\right] \approx \omega\left(E_t\left[\frac{s_{t+4}}{\theta}\right]\right) + \frac{1}{2}\phi\left(E_t\left[\frac{s_{t+4}}{\theta}\right]\right) \cdot Var\left[\frac{s_{t+4}}{\theta}\right].$$

It can be shown that the conditional expectation of the shadow rate is affine in states, and that the conditional variance is even constant (i.e. not depending on states) given the linear and Gaussian model for s_t. That is,

$$E_t\left[\frac{s_{t+4}}{\theta}\right] = A_4 + B_4'\xi_t \qquad \text{and} \qquad Var\left[\frac{s_{t+4}}{\theta}\right] = V_4,$$

where A_4, B_4 and V_4 are functions of the autoregressive process parameters of our state process, θ and δ_1.

We are now ready to define the approximate measurement equation for the short-term interest rate survey

$$E_t^s y_{t+4}(1) = E_t y_{t+4}(1) + u_t^{s,sr} \approx \theta\omega(A_4 + B_4'\xi_t) + \frac{1}{2}\theta\phi\big(A_4 + B_4'\xi_t\big) \cdot V_4 \equiv \tilde{Z}^s(\xi_t) + u_t^{s,sr}, \quad \text{(I.26)}$$

with corresponding Jacobian

$$\frac{d\tilde{Z}^s(\xi_t)}{d\xi} = \theta\Phi\big(A_4 + B_4'\xi_t\big)B_4' - \frac{1}{2}\theta V_4(A_4 + B_4'\xi_t)\phi\big(A_4 + B_4'\xi_t\big)B_4',$$

where the derivative employs the fact that $\phi'(x) = -x\phi(x)$.

J Additional robustness checks

J.1 Estimation in pseudo real-time

In this section, we analyze how the real-time estimates of the latent states and their uncertainty evolve over time. The focus is on r_t^* and its estimation uncertainty. To start, we estimate the model using the sample 1961Q4–1999Q4. Subsequently, we expand the sample by one quarter at the time until 2019Q4, and reestimate the model in pseudo-real time. This gives us 81 smoothed point estimates of r_t^* for each quarter between 1961Q4–1999Q4 (each indexed by the specific vintage) and one less per quarter going forward in time, until a single point estimate for

2019Q4. We do not account for data revisions. The priors are unchanged through this exercise. The left panel of Figure J.1 shows the posterior median estimates of r_t^*. As evident in the figure, the estimates are very robust over time, with limited variation in the posterior median point estimate of r_t^* for shorter samples. The right panel of Figure J.1 shows the respective width of the 95th-5th interpercentile range for each of the different vintages. The solid black line indicates the estimation uncertainty of the full sample version. The red crosses, in turn, mark the 95th-5th interpercentile range for the last estimate in each vintage. These are on average 0.22 percentage points above the full sample range, suggesting a modest decline in estimation uncertainty with an increasing sample.

Figure J.1: r_t^* estimates and uncertainty in pseudo-real-time

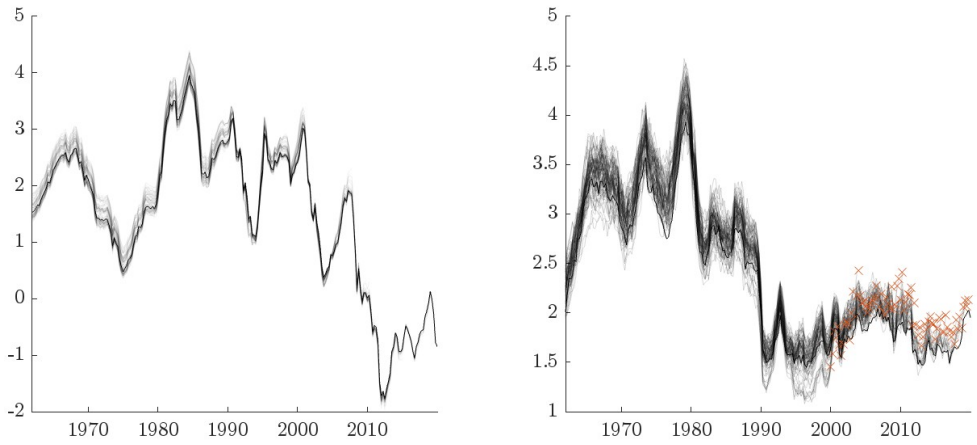

Note: The left panel plots the posterior median estimates of r_t^* with an expanding estimation window from 1961Q4–1999Q4 until 1961Q4–2019Q4. The right panel shows for each estimate the respective width of the 95th-5th interpercentile range.

J.2 Model with only short-term rate

As discussed in Section 4.1, the Holston et al. (2017) model is not "closed" as it treats the actual short-term real rate as exogenous. Given the dynamics of the inflation rate and an assumption on how inflation expectations are formed, closing the HLW model requires a specification of the nominal short-term interest rate. In the main body of this paper, we do so using an arbitrage-free term structure model, effectively specifying the entire nominal yield curve, with the aim of capturing the dual macro-finance role of equilibrium real rate. Yet, other alternatives are possible. Brand and Mazelis (2019), for instance, close the model by specifying the nominal interest rate as a function of inflation and output gap deviations from

their respective targets consistent with a Taylor (1993)-type reaction function. Arguably, an even simpler approach is to merely decompose the nominal short-term rate, $y_t(1) \equiv i_t$, into its trend component $i_t^* = r_t^* + \pi_t^*$, and a stationary cycle. To analyze how the specification of the short-term rate dynamics and the inclusion of multiple yields affects the estimate of r_t^*, we estimate a model version that replaces equation (8) of the main text with the following specification for the short-term nominal interest rate:

$$\begin{aligned} i_t =& r_t + E_t\pi_{t+1}, \\ =& r_t^* + \tilde{r}_t + \pi_t^* + E_t\tilde{\pi}_{t+1}, \\ =& r_t^* + \tilde{r}_t + \pi_t^* + b_1\tilde{\pi}_t + b_2\tilde{x}_t, \end{aligned} \tag{J.27}$$

where the last equality follows from equation (4) of the main text. The key difference to the baseline model is that the real rate gap, $\tilde{r}_t$, is assumed to follow a stationary first-order autoregressive process,

$$\tilde{r}_t = a_r\tilde{r}_{t-1} + \epsilon_t^r, \qquad \epsilon_t^r \sim \mathcal{N}(0, \sigma_r^2). \tag{J.28}$$

instead of being implicitly determined by the yield curve factors as in equation (18). For the estimation, we impose a Normal-Inverse-Gamma prior on (a_r, σ_r^2).[35]

Figure J.2: Comparison of latent states: short-rate-only model vs. baseline model

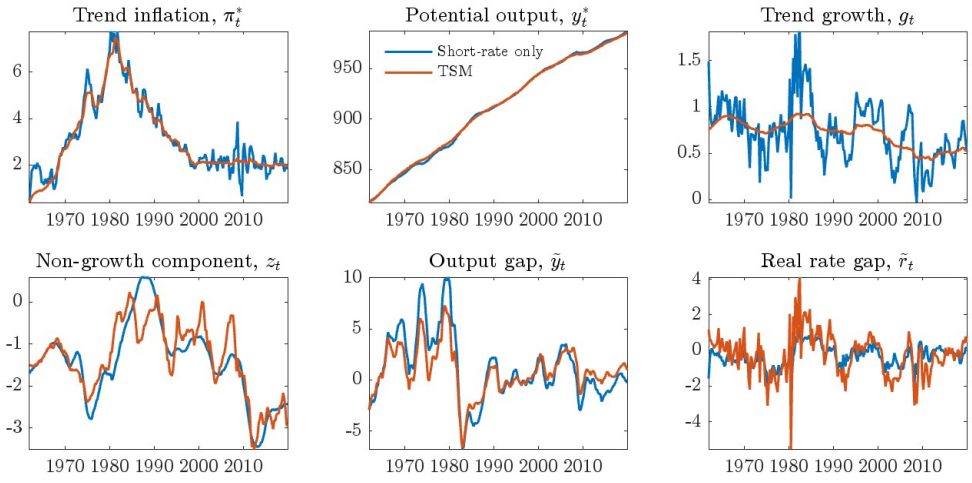

Note: Posterior median states of the short-rate-only model in blue and of the baseline term structure model (denoted "TSM") in red.

[35]Specifically, the prior for coefficient a_r is centered around 0.5 with a wide standard deviation of 0.25 and the prior shape and scale parameters for the innovations variance, σ_r^2, are 4 and 2, respectively.

However, in this agnostic setup, we run into econometric instability as too many draws from the conditional posterior of the coefficient of the lagged inflation gap in the Phillips curve, b_1 – which becomes an eigenvalue of the system – exceed the unit root. We therefore tighten the prior by choosing a very small prior standard deviation of 0.025 around the prior mean; ten times smaller than in our baseline. The resulting posterior estimates of the model's coefficients are similar to our baseline model. Yet, as can be seen in Figure J.2, the resulting posterior median estimates of latent states – in particular for trend inflation, π_t^*, and trend growth, g_t – are more volatile. This increased volatility carries over to the estimates of r_t^* as can be seen in the left-hand side of Figure J.3, suggesting that the model has more difficulties in decomposing real rates into their cyclical and trend components. Despite tighter priors and fewer latent states, overall estimation uncertainty for r_t^*, as measured by the width of the 90% credible set, is substantially higher in the first half of the sample. Only after the Great Moderation, when estimation uncertainty declines sharply in both models, the average width of the 90% credible set of the short-rate only model falls below that of our baseline specification.[36] On average over the sample, the estimation uncertainty is slightly smaller in the baseline model.

Figure J.3: Natural rate of interest and estimation uncertainty: short-rate-only model vs. baseline model

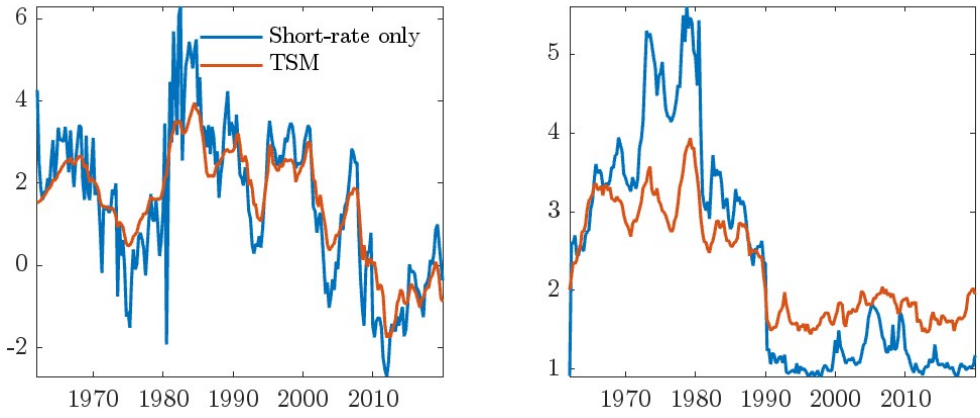

Note: The left panel compares the posterior median estimates of r_t^* from the short-rate-only model (blue) with our baseline term structure model (red). The panel on the right shows the respective 95th-5th interpercentile range of r_t^* as a measure of estimation uncertainty.

[36] Note that the marked decline in the IPR during the Great Moderation also aligns with the availability of the Consensus Economics interest survey.

J.3 A generalized affine no-arbitrage term structure specification

The arbitrage-free affine Nelson-Siegel (AFNS) set-up for the yield curve has a very parsimonious structure, as all factor loadings of yields depend on a single free parameter, λ. As shown in Appendix B, the factor loadings can be derived from no-arbitrage pricing equations. Joslin et al. (2011b) expound how the specific restrictions on risk-neutral model dynamics, especially the form of $\Phi^{\mathbb{Q}}_{uu}$, equation (B.15), are obtained starting from the canonical JSZ representation of the risk-neutral autoregressive matrix with two distinct eigenvalues, i.e. one appearing once, the other appearing as a pair:[37]

$$\tilde{\Phi}^{\mathbb{Q}}_{uu} = \begin{pmatrix} \lambda_0 & 0 & 0 \\ 0 & \lambda & 1 \\ 0 & 0 & \lambda \end{pmatrix}$$

This section offers yet another robustness check of our main results by generalizing the affine Nelson-Siegel setup. We keep the partitioning and reshuffling of the factor vector as in section B, i.e. we work with $F_t = (L_t, \bar{\xi}_t)$, where L_t is the level factor and $\bar{\xi}$ is a reshuffling ($\tilde{L}_t$ put after S_t and C_t) of the original state vector ξ.

The generalization will affect the specific parametrization of the risk-neutral autoregressive matrix $\Phi^{\mathbb{Q}}_{uu}$, i.e. the upper-left block of the overall autoregressive matrix as in equation (B.12). As is well known in the literature, an arbitrary (full) $\Phi^{\mathbb{Q}}_{uu}$ matrix does not make sense as it is not identifiable. We rather start again with the canonical JSZ representation, this time allowing for three distinct eigenvalues in $\Phi^{\mathbb{Q}}_{uu}$, leading to the structure

$$\Phi^{\mathbb{Q}}_{uu} = \begin{pmatrix} \lambda_0 & 0 & 0 \\ 0 & \lambda_1 & 0 \\ 0 & 0 & \lambda_2 \end{pmatrix}. \tag{J.29}$$

We set again $\lambda_0 = 1$ in order to preserve the interpretation of the first factor as a level factor, with its trend component related to r^*_t. We also stick to the factor labels as L_t, S_t and C_t, even though the different parametrization of $\Phi^{\mathbb{Q}}_{uu}$ implies that the narrow interpretation of the third factor as 'curvature' will not be applicable anymore.

We also keep $c^{\mathbb{Q}}_u = 0$, and set $\delta_u = (1, 1, 1)'$ and $\delta_0 = -\bar{S} - \bar{C}$. This leaves us with two

[37] The 1 appearing as (2,3) element in $\tilde{\Phi}^{\mathbb{Q}}_{uu}$ is due to the Jordan form in the standard JSZ representation with two repeated eigenvalues. It is absent, i.e. the matrix is diagonal, in the case of three distinct eigenvalues as chosen for our generalized case below.

free parameters, λ_1 and λ_2, instead of one as in our baseline arbitrage-free affine Nelson-Siegel (AFNS) case.

Also in this case, the solution to the difference equation for the factor loadings $b_u(\tau)$ (for bond *prices*) is given in closed-form,

$$b_u(\tau) = \left[-\tau, -\frac{1-\lambda_1^\tau}{1-\lambda_1}, -\frac{1-\lambda_2^\tau}{1-\lambda_2}\right] \tag{J.30}$$

with yield loadings

$$\mathcal{B}_u(\tau) = -\frac{1}{\tau} b_u(\tau). \tag{J.31}$$

Our choice of $\delta_0 = -\bar{S} - \bar{C}$ implies that $\lim_{h\to\infty} E_t i_{t+h} = L_t^*$ as in the baseline case.

Our state space representation, see Annex section A.1, is little affected by this generalization. Recall that the measurement equation is $\zeta_t = \gamma + \mathbf{C}\xi_t + \mathbf{D}u_t$. As before, the first K elements of γ are $\gamma(k) = \mathcal{A}(\tau_k)$ for $k = 1, \ldots, K$, with $\mathcal{A}(\tau_k) = -\frac{a(\tau_k)}{\tau_k}$, just that the difference equation (B.13) is now based on the new $b(\tau)$. Likewise, the upper left block of the $\mathbf{C}$ matrix in (A.6) associated with yields becomes

$$\mathbf{C}_{[1:K,1:3]} = \begin{pmatrix} \mathcal{B}_u(\tau_1)' \\ \vdots \\ \mathcal{B}_u(\tau_K)' \end{pmatrix},$$

where $\mathcal{B}_u(\tau_k)$ are now determined via (J.30)-(J.31).[38]

Also the state vector ξ_t and its law of motion remains unchanged. Yet given that δ_0 and δ_1 in the short-term interest rate equation $i_t = \delta_0 + \delta' F_t$ are different from the AFNS case, the intercept and loadings on the (lagged) slope and curvature factors in the IS curve change.

The estimation follows the same structure as in the baseline case only that the random-walk MH step for drawing the AFNS parameter λ (see section D) is replaced by an MH step that draws the two parameters λ_1 and λ_2 from an ordered random walk in order to avoid both eigenvalues to cross each other and flip the corresponding latent states. As prior, we choose a beta distribution for λ_1 and λ_2 which ensures that both values remain within $(0, 1)$.[39]

[38] As for the AFNS case in section B, the derivation of the generalized pricing equations works with the reshuffled and extended state vector that has the overall level factor in first position. However, the state space model can take over the loadings as they stand as the first element of the state vector is the *cyclical* level factor $\tilde{L}$ with a loading coefficient of unity. The other yield loadings for the level factor are then appearing later in the C matrix: with unity on g and π^*, and with a loading of 4 on g, together making a unity loading on L^*.

[39] We further reject any proposal $\lambda_1 > 0.98$ to ensure a strictly stationary second eigenvalue. The assumption

The posterior densities for λ_1 and λ_2 turn out to have a median of 0.956 and 0.607, respectively, and are precisely estimated, see Figure J.4 below.

Figure J.4: Posterior distribution of the second and third eigenvalues of $\Phi^{\mathbb{Q}}_{uu}$

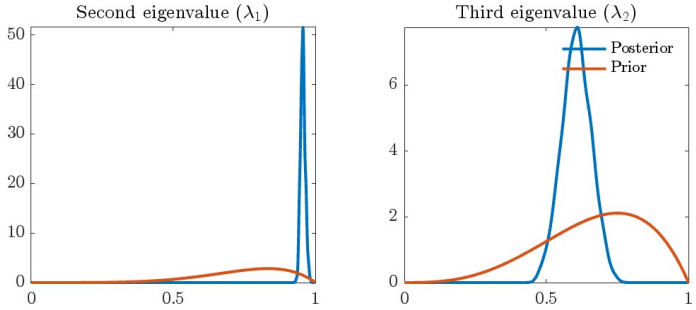

Note: The figure shows the posterior distribution of the second (left) and third (right) eigenvalue of the $\Phi^{\mathbb{Q}}_{uu}$ matrix in the generalized term structure model. The prior follows a β-distribution with shape and scale parameters $(6, 2)$ and $(4, 2)$, respectively.

Figure J.5 plots estimated factors under the generalized term structure model (GTSM) specification (blue) in comparison with the baseline AFNS case (red). Macro factors remain virtually unchanged, implying that also $r^*_t = 4g_t + z_t$ (not shown) remains essentially the same. Also the cyclical level factor for the GTSM shows very similar dynamics compared to the AFNS case. As mentioned before, the second and third factors now have different interpretations (we stick to the AFNS labels "slope" and "curvature" though) due to the different factor loadings, so they are not directly comparable but the slope factor shows similar dynamics under both specifications.

The fit to the yield curve is similar under both specifications, yet the root mean squared fitting error is lower by one or two basis points for the GTSM across maturities, see Table J.1. As an overall measure of fit across observable variables, we compute the marginal likelihood, and the GTSM has an edge over the baseline model also according to this criterion.

Model-implied five-year interest rate expectations five years ahead are closely correlated. However, the GTSM expectations are a bit lower. Accordingly, term premia are somewhat higher for the GTSM specification, but show very similar dynamics compared to the AFNS baseline.

Overall, making the yield curve pricing module more flexible compared to the one-parameter

is that the level factor remains $I(1)$ under the $\mathbb{Q}$ measure – as implied by the unity (1,1) element of $\Phi^{\mathbb{Q}}_{uu}$ – while the other factors are stationary. Choosing the proposal to "just" ensure $0 < \lambda_1, \lambda_2 < 1$ tends to lead to posterior densities that are similar to those obtained for our choice, but the greater proximity to the unit-root case renders the sampling (numerically) unstable. The ordering further ensures $\lambda_1 > \lambda_2$.

Figure J.5: Comparison of latent states: Generalized TSM vs. AFNS baseline

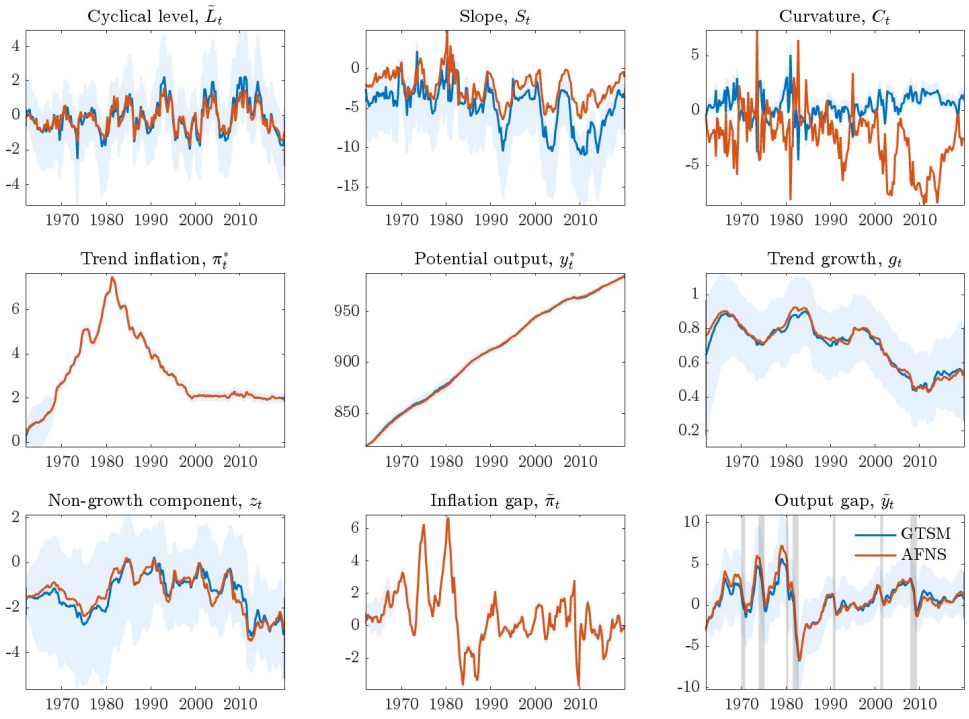

Note: Posterior median state estimates of the generalized term structure model in blue, with its 90% credible set, and posterior median state estimates of the baseline AFNS model in red.

Nelson-Siegel setting leads to a slightly better fit of the yield curve, it leaves relevant macro factors essentially unchanged, while term premia evolutions differ somewhat in levels but show very similar dynamics (see Figure J.6). As the (arbitrage-free) dynamic Nelson-Siegel set up is so prominent in the empirical macro-finance literature, we consider it useful to keep that specification as our baseline, rendering comparison to related studies more straightforward than using the generalized model.

J.4 Stochastic volatility in the IS and Phillips curve

In this section, we extend the model to allow for stochastic volatility in the IS and Phillips curve, i.e. we allow the standard deviations of the error terms in equations (1) and (4) of the main text, $\sigma_t^{\tilde{x}}$ and $\sigma_t^{\tilde{\pi}}$, to vary over time. Specifically, let the IS and Phillips curve be given:

$$\tilde{x}_t = a_1\tilde{x}_{t-1} + a_2\tilde{x}_{t-2} + a_3\big(\tilde{r}_{t-1} + \tilde{r}_{t-2}\big) + \sqrt{\exp(\ln h_t^{\tilde{x}})}\epsilon_t^{\tilde{x}},$$

Figure J.6: Comparison of forward rate expectations and term premium: Generalized TSM vs. AFNS baseline

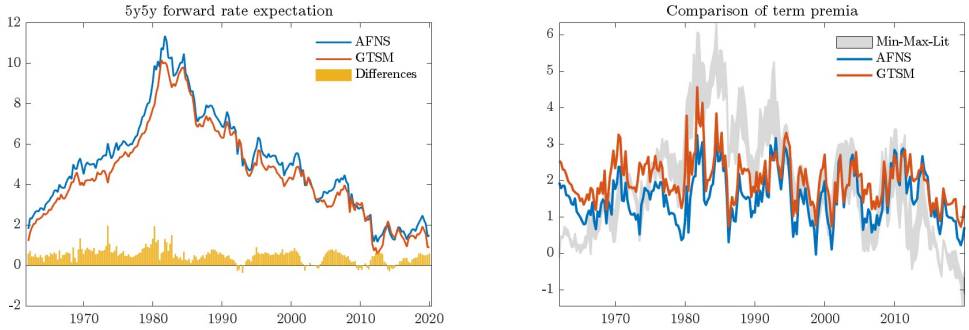

Note: The left panel compares the 5-year-forward-5-year-ahead average expected short-term rate between the AFNS and generalized term structure model version. Right panel shows the corresponding 5y5y forward term premium estimates relative to the min-max range of conventional estimates from the literature.

and

$$\tilde{\pi}_t = b_1\tilde{\pi}_{t-1} + b_2\tilde{x}_{t-1} + \sqrt{\exp(\ln h_t^{\tilde{\pi}})}\epsilon_t^{\tilde{\pi}},$$

respectively. h_t^k denotes the time-varying variance, with $\epsilon_t^k \sim \mathcal{N}(0,1)$, for $k = \{\tilde{x}, \tilde{\pi}\}$. Jacquier et al. (1994) suggest to apply an independence MH algorithm at each point in time to sample from the conditional distribution of h_t^k which is given by $f(h_t^k|h_{-t}^k, \xi_t)$ where the subscript $-t$ denotes all other dates than t. By further specifying a random walk transition equation for $\ln h_t^k$,

$$\ln h_t^k = \ln h_{t-1}^k + \nu_t^k, \qquad \nu_t^k \sim \mathcal{N}(0, g_k),$$

the conditional distribution can be simplified as $f(h_t^k|h_{-t}^k, \xi_t) = f(h_t^k|h_{t-1}^k, h_{t+1}^k, \xi_t)$. Our priors for h_k are $p(\ln h_t^k) \sim \mathcal{N}(\bar{\mu_k}, \bar{\sigma_k})$, where $(\bar{\mu_k}, \bar{\sigma_k})$ are set to the (log) posterior of the baseline model (see Table 1 in the main text). We further specify an Inverse Gamma prior for g_k, i.e. $p(g) \sim \Gamma^{-1}(a_0, b_0)$ with prior scale and shape $a_0 = 50$ and $b_0 = 0.5$, respectively. The implementation follows Jacquier et al. (1994) and is a straight forward extension of our Gibbs sampler with a sequential independence Metropolis Hastings (MH) to draw h_t^k and g before step 1. in the algorithm of Section D.

The top panels in Figure J.4 show that the posterior variances are precisely estimated, despite further increasing the complexity of the model. The variance associated with the residuals in the IS curve is elevated during the 1970s and 1980s and falls through the Great Moderation. The same holds for the residual variances in the Phillips curve. Yet the latter also peaks in 2009-

10, reflecting the sharp deflationary impulse of the GFC. The posterior median of the constant volatility model lies in between.

While a time-varying specification for the variances is arguably more plausible from an economic perspective, the middle and bottom panels suggest that the output and inflation gap estimates are barely affected. As a result, differences in the posterior median estimate of r_t^* are also negligible. Differences in the estimation uncertainty can be sizable at times, but do not persist. If anything, the constant volatility model may imply a somewhat lower estimation uncertainty after the Great Moderation.

J.5 Model with trivariate VAR for the stationary yield curve factors

In this section, we generalize the model by assuming that the stationary yield curve factors $(\tilde{L}_t, S_t, C_t)$ jointly follow a trivariate VAR, with the output and inflation gap as exogenous variables. For this purpose, exchange equations (11)-(13) in the main text with the following equation:

$$\begin{pmatrix} \tilde{L}_t \\ S_t \\ C_t \end{pmatrix} = \begin{pmatrix} a_{10} \\ a_{20} \\ a_{30} \end{pmatrix} + \begin{pmatrix} a_{11} & a_{12} & a_{13} \\ a_{21} & a_{22} & a_{23} \\ a_{31} & a_{32} & a_{33} \end{pmatrix} \begin{pmatrix} \tilde{L}_{t-1} \\ S_{t-1} \\ C_{t-1} \end{pmatrix} + \begin{pmatrix} a_{14} & a_{15} \\ a_{24} & a_{25} \\ a_{34} & a_{35} \end{pmatrix} \begin{pmatrix} \tilde{\pi}_{t-1} \\ \tilde{y}_{t-1} \end{pmatrix} + \mathbf{I} \begin{pmatrix} \varepsilon_t^{\tilde{L}} \\ \varepsilon_t^{S} \\ \varepsilon_t^{C} \end{pmatrix}. \tag{J.32}$$

We assume a Normal-Inverse Wishart prior that mimics the prior on the baseline specification. Specifically, for slope and curvature, the prior assumes each to follow a persistent AR(1) with intercept, with the priors being equally tight on coefficients and variances. For the cyclical level factor, the AR(1) coefficient is centered around 0.5 with a standard deviation of 0.25. To further ensure consistency with the zero-mean property of the cyclical level factor, we a priori impose that the intercept a_{10} is zero.

Table J.2 presents the parameter estimates. Overall, parameter estimates appear fairly robust and – as further supported by Figure J.8 – this modeling choice does not affect the posterior median estimates of the smoothed states.

J.6 Looser prior on the variance of trend growth

As laid out in the main text, our baseline model assumes a relatively tight prior on the variance of trend growth to ensure smooth dynamics in the growth of potential output. In this section, we present the results for using a looser prior on the variance of trend growth. Specifically, we re-estimate the model, assuming a prior distribution of $\Gamma^{-1}(100, 2)$ for the variance of trend growth. This prior implies a prior mean that is nearly fifteen times larger than in our baseline specification, and a variance around that (higher) mean which is more than twenty times larger. As a result of the less informative prior, trend growth g_t absorbs some of the cyclical dynamics in output (see left panel in Figure J.9), rendering the resulting output gap less persistent. Estimates for r_t^*, however, remain unaffected (see right panel in Figure J.9).

J.7 Coefficients of expected growth on the natural rate

As discussed in the main text, the Laubach and Williams framework imposes a fixed loading of the expected quarterly trend growth on the (annualized) natural rate of interest in Equation (3)in the main text. However, some recent studies, including Lunsford and West (2019), have highlighted the weak empirical relationship between real rates and (trend) growth. This section presents a version of the model that relaxes this assumption by additionally estimating the coefficient α in

$$r_t^* = \alpha g_t + z_t. \tag{J.33}$$

We assume a priori that α is normally distributed around 4 – the value chosen by Laubach and Williams (2016) – with a wide variance $\sqrt{2}$, i.e. our prior for α is $p(\alpha_0) \sim \mathcal{N}(4, \sqrt{2})$. For the estimation, we add an additional random walk Metropolis Hastings step into the estimation algorithm with the scale parameter set to achieve an acceptance rate between 20-40%.

Figure J.10 shows the prior and posterior distribution. While the posterior median turns out to be lower than the value imposed by Laubach and Williams (2003, 2016), we find a significantly positive effect of expected real potential growth on trend real interest rates in line with standard theory that links real rates to productivity growth. Specifically, the posterior median is 2.74, with the 90% credible set ranging from 1.4 to 4.4. In contrast to Lunsford and West (2019), our specification, following Laubach and Williams (2003) and later variants, assumes such a link in the long-run, thus stripping cyclical variation in both real rates and economic growth (or productivity) from their respective long-run trends that could create econometric challenges

arising from e.g. the endogeneity of both. Our estimate of r_t^* remains unchanged.

J.8 Coefficients of the real rate gap in the IS curve

In our specification of the IS curve that originates from the Laubach and Williams (2003, 2016) model, the two lags of the real rate gap load on the output gap with the same coefficient. As a robustness check, we relaxed this assumption and instead estimate the model allowing for the two lags of the real rate gap to affect the output gap differently, thus exchanging equation (1) in the main text with

$$\tilde{x}_t = a_1\tilde{x}_{t-1} + a_2\tilde{x}_{t-2} + a_3\tilde{r}_{t-1} + a_4\tilde{r}_{t-2} + \varepsilon_t^{\tilde{x}}. \tag{J.34}$$

The left panel of Figure J.11 plots the posterior distributions for the parameter in our baseline model and compares it with the respective posterior distributions of the case in which the parameters are allowed to be different. The posterior distributions of the parameters of the first and second lag of the real rate gap largely fall on top of each other, with negligible differences in the medians ($\bar{a}_3 = -0.094$ vs. $\bar{a}_4 = -0.100$). Both, in turn, are hardly different from the posterior distribution of our baseline estimation, with an overall comparable estimation uncertainty.

Finally, and most importantly, the posterior estimates of the latent states are not affected as shown in the right hand side panel of Figure J.11 for our main object of interest, r_t^*.

Table J.1: Root mean squared fitting errors across maturities (in percentage points)

Maturity (in quarter)	τ =2	τ =3	τ =4	τ =8	τ =12	τ =16	τ =20	τ =24	τ =28	τ =32	τ =36	τ =40
AFNS model	0.12	0.15	0.15	0.09	0.05	0.07	0.09	0.09	0.06	0.03	0.08	0.16
GTSM	0.11	0.14	0.13	0.08	0.05	0.06	0.08	0.07	0.05	0.03	0.06	0.13

Table J.2: Posterior estimates of the stationary yield curve parameter

	Baseline			**trivariate VAR**		
Parameter	5%	Median	95%	5%	Median	95%
a_{10}	-	-	-	-0.347	-0.129	0.055
a_{11}	0.212	0.508	0.825	0.548	0.711	0.858
a_{12}	-	-	-	-0.124	-0.045	0.030
a_{13}	-	-	-	-0.087	-0.055	-0.023
a_{14}	-	-	-	-0.002	0.057	0.112
a_{15}	-	-	-	-0.143	-0.072	-0.011
a_{20}	-0.925	-0.539	-0.215	-1.299	-0.827	-0.432
a_{21}	-	-	-	-0.693	-0.430	-0.099
a_{22}	0.572	0.689	0.787	0.365	0.534	0.703
a_{23}	0.075	0.135	0.192	0.028	0.092	0.167
a_{24}	-0.121	-0.006	0.114	-0.103	0.043	0.192
a_{25}	0.073	0.150	0.246	-0.005	0.106	0.220
a_{30}	-0.647	-0.104	0.367	-0.288	0.221	0.742
a_{31}	-	-	-	-0.022	0.409	0.865
a_{32}	0.182	0.328	0.487	0.236	0.444	0.669
a_{33}	0.529	0.622	0.706	0.576	0.670	0.752
a_{34}	-0.192	-0.037	0.126	-0.282	-0.111	0.047
a_{35}	-0.281	-0.129	0.003	-0.171	-0.017	0.126

Figure J.7: Estimation results of the model with stochastic volatility

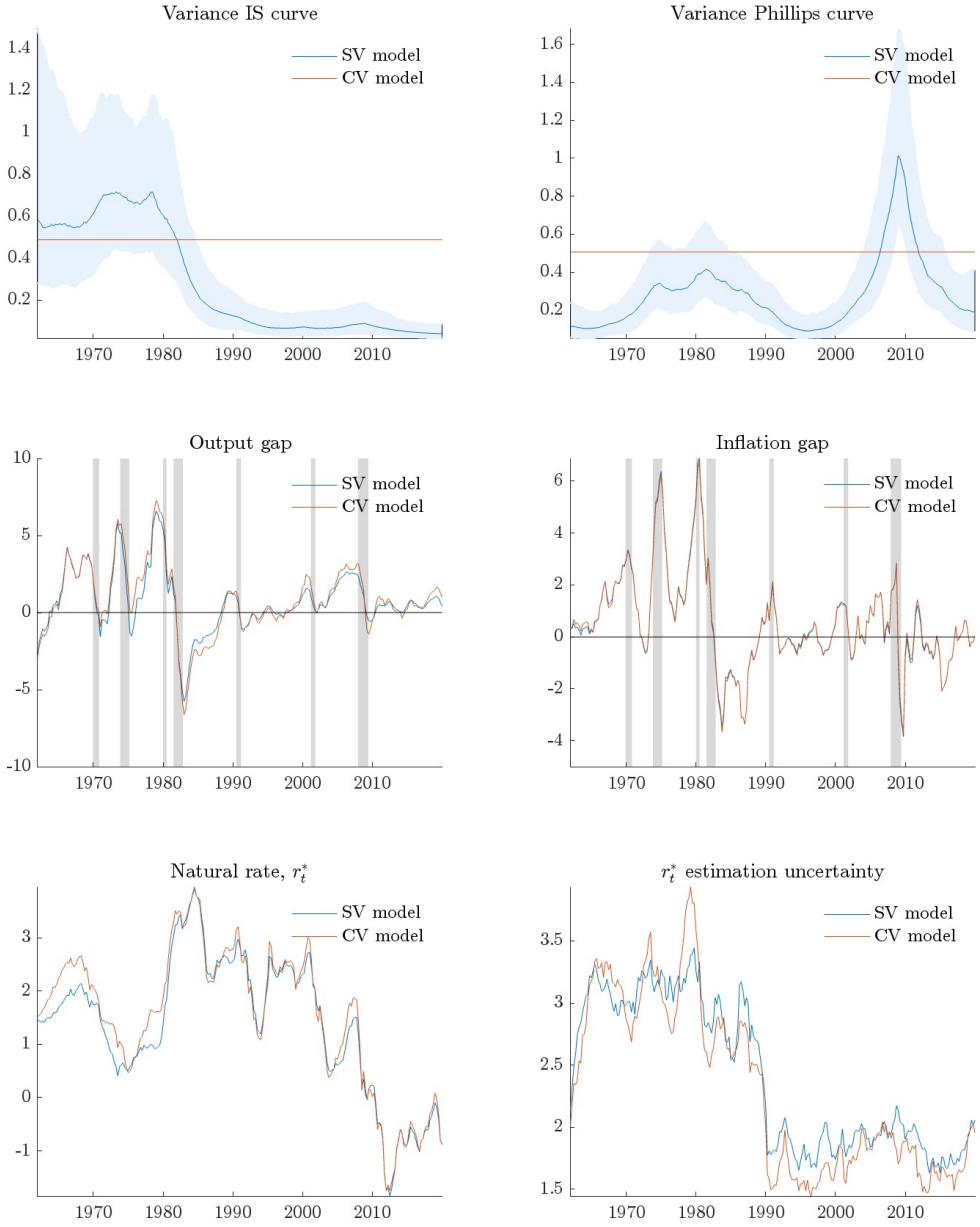

Note: The top row shows the posterior estimates of the time-varying variances of the IS and Phillips curve. The middle panel compares the output and inflation gap of the stochastic versus constant (baseline) volatility model. The bottom row compares the posterior median r_t^* estimate and its 95th-5th interpercentile range of the stochastic vs. constant volatility model.

Figure J.8: Comparison of latent states: model with trivariate VAR for the stationary yield curve factors vs. baseline model

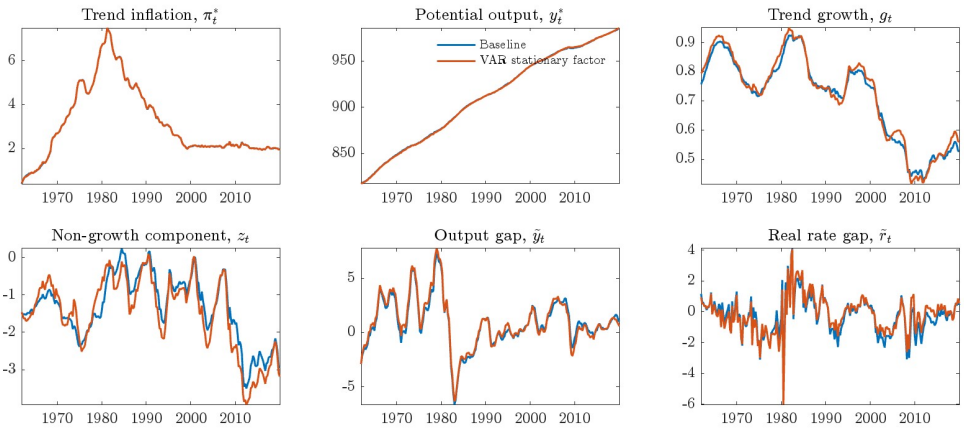

Note: Posterior median state estimates of model with a trivariate VAR for the stationary yield curve factors in blue and that of the baseline model in red.

Figure J.9: Looser prior on trend growth: effect on r_t^*

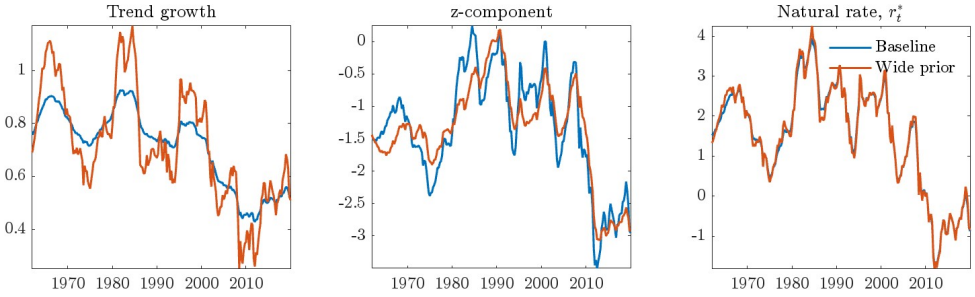

Note: The figure shows r_t^* and its components from our baseline estimation and compares it to the case of a looser prior on the variance of trend growth equal to $\Gamma^{-1}(100, 2)$.

Figure J.10: Prior and posterior distribution of α

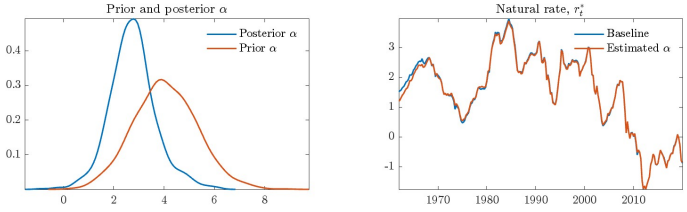

Note: The figure shows the prior and posterior densities of the parameter α in Equation (J.33). In the baseline model, α is fixed to 4 as in Laubach and Williams (2003, 2016).

Figure J.11: Posterior plots and natural rate estimates

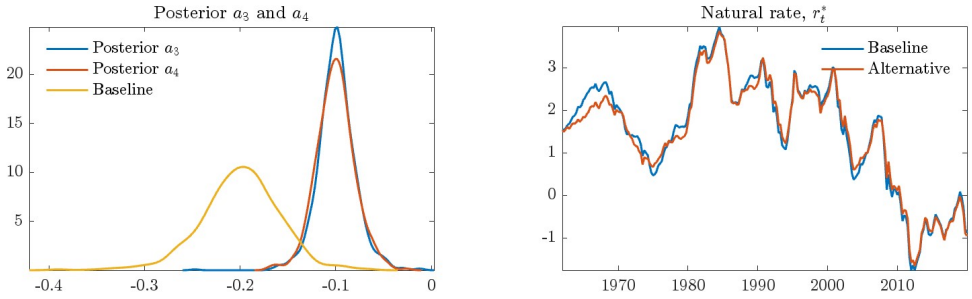

Note: The left panel shows the posterior distributions of the parameter a_3 and a_4 for the model version in which the two are allowed to differ. The right panel compares the resulting posterior median r_t^* estimate to our baseline.

Acknowledgements

We are grateful for suggestions by and discussions with Daniel Buncic, Lawrence Christiano, Marco Del Negro, Michael Kiley, Leonardo Melosi, Elmar Mertens, Adrian Penalver, Paolo Pesenti, Jean-Paul Renne, Glenn Rudebusch, Nicolas Sander and Bernd Schwaab. Finally, we also thank seminar participants at De Nederlandsche Bank, the National Bank of Belgium, Toulouse School of Economics and Banque de France, the European Central Bank, as well as participants of the joint DNB-ECB workshop on the natural rate of interest in Amsterdam, 2019, the Computational Economics and Finance conference in Ottawa, 2019, the Computational Finance and Econometrics conference in London, 2019, the Meeting of European Economic Association 2020, the annual meeting of the Verein für Socialpolitik, 2020, the joint EABCN, Banque de France and UPF Conference on Empirical Advances in Monetary Policy, 2020, and the Bundesbank, EABCN and CEPR conference in Eltville on Challenges in Empirical Macroeconomics, 2022, the 16th Dynare Conference in Lancaster, the LFin seminar at UCLouvain, 2023 and the Sailing the Macro Conference in Ortygia, 2023. Special thanks to Michael Bauer for sharing the Bauer and Rudebusch (2020) term premium and i* estimates with us.

Claus Brand
European Central Bank, Frankfurt am Main, Germany; email: claus.brand@ecb.europa.eu

Gavin Goy
De Nederlandsche Bank, Amsterdam, The Netherlands; email: g.w.goy@dnb.nl

Wolfgang Lemke
European Central Bank, Frankfurt am Main, Germany; email: wolfgang.lemke@ecb.europa.eu

Postal address 60640 Frankfurt am Main, Germany
Telephone +49 69 1344 0
Website www.ecb.europa.eu

PDF ISBN 978-92-899-7528-5 ISSN 1725-2806 doi:10.2866/0150284 QB-01-25-274-EN-N